Molecular Structure Refinement Based on Residual Dipolar Couplings: A Comparison of the Molecular Rotational-Sampling Method with the Alignment-Tensor Approach

Maria Pechlaner[#], Wilfred F. van Gunsteren[#], Lorna J. Smith[†], Bartosz Stankiewicz[&] Lukas N. Wirz[§] and Niels Hansen[&*]

[†]Department of Chemistry, Inorganic Chemistry Laboratory, University of Oxford, South Parks Road, Oxford, OX1 3QR, UK,

[#]Institute for Molecular Physical Science, Swiss Federal Institute of Technology, ETH, CH-8093 Zurich, Switzerland,

[&]Institute of Thermodynamics and Thermal Process Engineering, University of Stuttgart, D-70569 Stuttgart, Germany

[§]Department of Chemistry, University of Helsinki, P.O. Box 55, A.I. Virtasen Aukio 1, FIN-00014 Helsinki, Finland

[*]Corresponding author. Electronic mail: hansen@itt.uni-stuttgart.de

Version/Date: 09-05-2024

For submission to J. Chem. Inf. Model.

Keywords

Structure refinement, nuclear magnetic resonance, residual dipolar couplings, rotational sampling, alignment tensor, flexibility, averaging, restraining force, orientation-biased molecular distribution

Abstract

In NMR experiments, residual dipolar couplings (RDCs) in a molecule can be measured by averaging the dipolar couplings (DCs) over the rotational motion of a molecule in an environment that induces a slight anisotropic orientation distribution of the molecule. Since the shape of the anisotropic distribution cannot be measured, it is standard practice to use a particular orientation distribution of the molecule with respect to the magnetic field, in the form of a so-called alignment tensor (*AT*), to calculate RDC-values for the molecule. Since the same alignment tensor is commonly used to calculate the different RDCs of a molecule, this approach rests on the assumptions that the rotational motion of the molecule is decoupled from its internal motions and that the molecule is rigid. The validity of these two assumptions is investigated for a small, simple molecule, using a relatively rigid atomic interaction function or force field and a more flexible one. By simulating the molecule using an orientation-biasing force an anisotropic rotational distribution can be generated, for which RDCs can be obtained. Using these RDCs as target RDCs when applying one of the two approaches of structure refinement based on RDCs, it can be investigated how well the target RDCs are approximated in the RDC restraining and whether the corresponding non-uniform orientation distribution is reproduced.

For the relatively rigid version of the molecule, the *AT* approach reproduces the target RDC-values, although the non-uniform orientation distribution of the angle $\theta_{ab,H}$ between the vector $\vec{r}_{ab}$ connecting two atoms *a* and *b* in the molecule and the vector representing

the direction of the magnetic field $\vec{H}$ as generated in the orientation-biasing simulation cannot be reproduced in the *AT* RDC-restraining simulation. For the relatively flexible version of the molecule, the *AT* approach fails to reproduce both the target RDC-values and the non-uniform orientation distribution. For bio-molecules with flexible parts the application of the *AT* approach is thus not recommended. Instead, a method based on sampling of the rotational and internal degrees of freedom of the molecule should be applied in molecular structure determination or refinement based on measured RDCs.

1. Introduction

During the past decades, structure determination of molecules in solution, that are biologically relevant, such as proteins, nucleic acids and carbohydrates, based on Nuclear Magnetic Resonance (NMR) spectroscopic measurements of a variety of observable quantities has become a standard technique in biochemistry and molecular biology[1-4]. Various observable quantities, such as Nuclear Overhauser enhancements (NOEs), ^3J-couplings or chemical shifts, only provide local structural information. In contrast, residual dipolar couplings (RDCs) do provide longer-range information in terms of the average (relative) direction of bond vectors throughout a molecule[5,6].

1.1. Residual dipolar couplings: definition

A dipolar coupling $D_{k_1k_2}$ or in short D_k between two nuclear spins k_1 and k_2 in a homogeneous magnetic field $\vec{H}$ depends on[7] (*i*) the length $r_{k_1k_2} \equiv |\vec{r}_{k_1k_2}|$ of the inter-nuclear vector $\vec{r}_{k_1k_2} \equiv \vec{r}_{k_1} - \vec{r}_{k_2}$, and (*ii*) the angle θ_k of this vector with the static magnetic field $\vec{H}$, e.g. $\cos(\theta_k) = (z_{k_1} - z_{k_2})/r_{k_1k_2}$ when $\vec{H}$ lies along the z-axis of the coordinate system, and

$$D_k = \frac{-\mu_0 h \gamma_{k_1} \gamma_{k_2}}{8\pi^3} \left(\frac{3\cos^2(\theta_k) - 1}{2r_k^3} \right) \quad . \tag{1}$$

Here, the short-hand notation $r_k \equiv r_{k_1k_2}$ is used, μ_0 is the magnetic permeability of vacuum $(\varepsilon_0 c^2)^{-1} = 4\pi\ 10^{-7}$ J s^2 / (C^2 m) or 1.9425913 10^{-8} kJ mol^{-1} ps^2 / (e^2 nm), h is Planck's constant, 6.626176 10^{-34} J s or 0.3990313 kJ mol^{-1} ps, and γ_i is the gyromagnetic ratio[8,9] of nucleus i. The constant and variable factors in Eq. (1) can be separated as follows,

$$D_k(t) = D_k^c \left(\frac{r^0}{r_{k_1 k_2}(t)} \right)^3 \left(\frac{1}{2}\left(3\cos^2\left(\theta_k(t)\right) - 1\right) \right) = D_k^c R_k(t) P_k(t) \quad (2)$$

with

$$D_k^c \equiv \frac{-\mu_0 h}{2\pi \left(r^0\right)^3} \left(\frac{\gamma_{k_1}}{2\pi} \right) \left(\frac{\gamma_{k_2}}{2\pi} \right) \ , \quad (3)$$

$$R_k(t) \equiv \left(\frac{r^0}{r_{k_1 k_2}(t)} \right)^3 , \quad (4)$$

$$P_k(t) \equiv \frac{1}{2}\left(3\cos^2\left(\theta_k(t)\right) - 1\right) \ . \quad (5)$$

The second-order Legendre function $P_k(\theta_k(t))$ has two zero's, at the so-called magic angles ($|\cos(\theta)| = 3^{-1/2}$) 55° and 125°, two maxima of 1 at 0° and 180°, and a minimum of -1/2 at 90°. It is symmetric around θ = 90°. Since the distance between nuclei k_1 and k_2 is generally of the order of 0.1 nm, one may choose r^0 = 0.1 nm, which yields $-\mu_0 h/(2\pi(r^0)^3)$ = -1.3252 10^{-10} J^2 s^3 C^{-2} m^{-4} or -1.2336 10^{-6} (kJ $mol^{-1})^2$ ps^3 e^{-2} nm^{-4}. Approximate values of the gyromagnetic ratio for some nuclei can be found in Refs.[8,9]. For an N-H pair of nuclei we find for example $D_k^c(^{14}N - ^1H)$ = -17.37 kHz and $D_k^c(^{15}N - ^1H)$ = +24.36 kHz. We note, however, that a dipolar coupling is also influenced by external factors, such as neighbouring nuclei[10]. Eq. (1) is thus an approximation.

In a measurement of RDCs the value of D_k in Eq. (1) is averaged over molecules and an experimentally determined time period. Since a dipolar coupling D_k generally involves atoms in a molecule that are covalently bound to each other or at a short distance, while the molecule contains many atoms, one may use the assumption that the fluctuation of the distance $r_{k_1 k_2}$ is not coupled to the rotational motion of the vector $\vec{r}_{k_1 k_2}$ with respect to the

magnetic field direction $\vec{H}$. So, the averaging of D_k may be separated into an average over $(r_{k_1k_2})^{-3}$ and one over the second-order Legendre function of θ_k,

$$\langle D_k \rangle = D_k^c \left\langle \left(\frac{r^0}{r_{k_1k_2}} \right)^3 \right\rangle \left\langle \left(\frac{1}{2}\left(3\cos^2(\theta_k) - 1\right) \right) \right\rangle \quad . \tag{6}$$

The average $\langle (r^0/r_{k_1k_2})^3 \rangle$ will be close to one in case $r_{k_1k_2}$ is a fluctuating bond length and r^0 a value close to its average. For an isotropically tumbling molecule the average over the function $P_k(\theta_k)$ will be zero,

$$\langle P_k(\theta_k) \rangle \equiv \left\langle \frac{1}{2}\left(3\cos^2(\theta_k) - 1\right) \right\rangle = 0 \quad , \tag{7}$$

leading to $\langle D_k \rangle = 0$.

However, if one would be able to introduce an anisotropy in the rotational tumbling of the molecule, one would have $\langle D_k \rangle \neq 0$, and the values of $\langle D_k \rangle$ would yield values of the averages $\langle P_k(\theta_k) \rangle$ and some information about values of the angles θ_k.

1.2. Anisotropy of the molecular rotational distribution

Experimentally, such an anisotropy can be induced in different ways[7], (*i*) using the paramagnetic susceptibility $\chi_r \equiv \mu_r$ - 1 of a molecule, (*ii*) using electrostatic interactions with a molecule, or (*iii*) by immersing the molecule in a medium that contains some order that will influence the angular distribution $P(\theta_k)$ of the angle θ_k of the *k*-th RDC-vector in the molecule with the magnetic field (z-axis). In this way, small values of $\langle D_k \rangle$, called *residual* dipolar couplings (*R*DCs), of the order of Hz, that is $10^3 - 10^4$ smaller than the values of the dipolar couplings D_k themselves, which are of the order of kHz, can be

obtained. Unfortunately, the size and shape of the experimentally induced anisotropy in the rotational distributions $P(\theta_k)$ cannot be measured. $P(\theta_k)$ is not an observable quantity. This anisotropy will be different for different media, leading to rather different $<D_k>$ values for different media[11].

1.3. The alignment-tensor approach

In the alignment-tensor (*AT*) approach, the orientation distribution of a molecule with respect to a magnetic-field direction is described[10] in terms of a basis set of five spherical harmonic functions of order 2. The real physical orientation distributions of the RDC-vectors, here generated using molecular dynamics (MD) or stochastic dynamics (SD) simulation of the motions of the molecule applying an orientation-biasing force, may, however, differ from the *AT* one described in terms of spherical harmonics of order 2.

In the *AT* approach the molecular rotational degrees of freedom of the molecule are not sampled in a simulation but represented by an orientation distribution of the molecule with respect to the magnetic field (e.g. the z-axis). This involves the assumption that the overall rotation of the molecule is decoupled from its internal motions. In addition, it is often assumed that the alignment or orientation distribution of the molecule has the same effect on different $<D_k>$ values (RDCs), i.e. that the molecule is rigid.

In the *AT* approach the unknown alignment distribution of the molecule is represented by a so-called 3 x 3 alignment tensor, which depends on 5 parameters, three (Euler) angles plus two non-spherical symmetry parameters for the molecule. The 3 x 3 tensor is symmetric and has trace zero, so it has only 5 independent tensor elements, which represent

the anisotropy of the rotational distribution in terms of the 5 coefficients a_m ($m = 1 - 5$) of the five spherical harmonic basis functions of order 2 (defined in section 2.4).

The 5 parameters determining the molecular alignment distribution can be determined in various ways.

1. Estimation (*i*) from the shape of the molecule[12], or (*ii*) from its moments of inertia[13], or (*iii*) from its gyration tensor[14], or (*iv*) from its hydrodynamic shape[15], or (*v*) from its alignment against a hypothetical wall, while considering its charge distribution[16].

2. Use of a given set of (measured, target) RDC values by optimising the agreement between the given and calculated RDCs of the set, which must contain at least five RDC values. This optimisation can be performed by a linear least-squares fit[10], by single-value decomposition, which is less efficient[17], or by molecular dynamics (MD), stochastic dynamics (SD) or Monte Carlo (MC) sampling of the domain of the five alignment-tensor parameters.

In the *AT* formalism, the motions of the molecule can be accounted for in three different ways.

1. Orientational constraints[18] or tensorial constraints[19] can be applied to sample a limited part of the rotational space of the molecule.

2. Generalised order parameters *S* for RDC-vectors may be defined, which represent the small amplitude directional variation of these RDC-vectors, e.g. with values in the range [0.7–0.9][20]. In the simulated annealing procedure for structure determination the *S*-value, which is taken equal for all RDCs, is allowed to vary in order to minimise *RMSD*(*D*-

D^0), the root-mean-square difference between the calculated (D) and target (D^0) RDC-values.

3. An alternative is the use of multiple conformations in structure refinement, in which two of more (N_c) are used with equal weights $1/N_c$ in the structure refinement procedure that minimises $RMSD(D\text{-}D^0)$[21,22].

The introduction of additional parameter or conformational degrees of freedom in structure refinement leads unavoidably to lower $RMSD(D\text{-}D^0)$-values. The mentioned extensions of the *AT* formalism allow for a representation of small amplitude motion of parts of the molecule, but are not able to reflect the physical dynamics of the motion and they ignore the statistical-mechanical Boltzmann (energy-dependent) weights of the different molecular configurations. This means that these extended *AT* approaches are expected to perform well for rigid molecules or when many structural restraints, i.e. NOE distance restraints, ^3J-coupling derived torsional-angle restraints and hydrogen-bond restraints are applied[21,22]. However, for flexible molecules in the absence of other restraints rigidifying the molecule these methods are not expected to perform well.

1.4. Sampling of the rotational degrees of freedom of a molecule

A recently proposed alternative approach (*MRS*: molecular rotational sampling)[23] to use measured RDC values for structure determination or refinement of molecules is based on sampling the molecular rotational degrees of freedom of a molecule by MD or SD simulation in combination with molecule-internal configurational averaging. It avoids the use of an alignment tensor, and thus avoids the assumption that the overall rotation of the

molecule is decoupled from its internal motions. It also avoids the assumption that the molecule is rigid and thus allows for molecular flexibility. MD or SD simulations are performed that are sufficiently long to sample the rotational distribution well, i.e. long enough to reduce the $<D_k>$ values, which should for infinite sampling (of a uniform rotational distribution) become zero, to beyond values that are about 10^{-3} to 10^{-4} of the values of D_k^c. Inclusion of a penalty function that drives the calculated RDCs toward the measured ones in the potential energy function of such a simulation then generates a conformational ensemble compatible with the given set of (measured) RDC values. As long as the RDC-restraining forces and energy are small compared to the forces and energy of the molecular model and force field used, the MD or SD simulations yield molecular conformations with the appropriate Boltzmann weights.

In the current article both approaches (*AT* and *MRS*) are applied to a small molecule, using a standard molecular force field and using a more flexible one, with the aim of investigating the effects of the limitations of the alignment-tensor approach, i.e. that the overall rotation of the molecule is decoupled from its internal motions and that the structural variability of the molecule is restricted.

2. RDCs as restraints in molecular simulation

2.1. Choice of restraining function

In analogy to the flat-bottom restraining function for NOEs, ^3J-couplings and S^2 order parameters[24], a simple RDC-restraining function, continuous with continuous derivative, is a quadratic one with a flat bottom that allows for a penalty-free range of deviations $2\Delta D^0$ of the average $<D_k>$ value or the instantaneous D_k value from its target (measured) value D_k^0, see Eqs. (16,17) of Ref.[23]. We note that since the GROMOS (Groningen Molecular Simulation) force fields[25-29] treat aliphatic CH_n moieties as united atoms, virtual atoms[26,,29,30] are to be used in case C_α-H_α RDCs are to be calculated.

2.2. Accounting for time-averaging

An RDC is intrinsically an averaged (over the rotation of the molecule) quantity, $<D_k>$, that cannot be linked to a single configuration. When restraining an averaged quantity, the averaging cannot be over the whole simulation period up till time point *t*, because the contribution of the current configuration at time *t* to the average would tend to zero for *t* approaching infinity. This implies that the restraining force, which can only be applied to the current configuration at time *t*, would also tend to zero for *t* approaching infinity. For this reason an exponential memory function[31,32] is used in the time-average $\overline{D_k}^t \equiv <D_k>_t$ that is used in the RDC-restraining function[23], with the memory relaxation time τ_D^{RDC} determining the averaging time period,

$$\overline{D_k\left(\vec{r}^{\,N}(t)\right)}^{t,\exp} = \left(\tau_D^{RDC}\left(1-\exp(-t/\tau_D^{RDC})\right)\right)^{-1}\int_0^t \exp(-(t-t')/\tau_D^{RDC})D_k(\vec{r}^{\,N}(t'))dt' . \qquad (8)$$

As discussed before, the averaging over the two time-dependent factors in Eq. (2) may be well approximated, due to the different relevant time scales, by a separation, see Eq. (6), so

$$\overline{D_k\left(\vec{r}^{\,N}(t)\right)}^{t} = D_k^c \overline{\left(\frac{r^0}{r_{k_1k_2}(t)}\right)^3}^{t} \overline{\left(\frac{1}{2}\left(3\cos^2\left(\theta_k(t)\right)-1\right)\right)}^{t} = D_k^c \quad \overline{R_k(t)}^{t} \quad \overline{P_k(t)}^{t}. \tag{9}$$

The two time-averaged quantities $\overline{R_k(t)}^{t}$ and $\overline{P_k(t)}^{t}$ in Eq. (9) are calculated in the above-mentioned damped-memory manner,

$$\overline{R_k\left(\vec{r}^{\,N}(t)\right)}^{t,\exp} = \left(\tau_r^{RDC}\left(1-\exp(-t/\tau_r^{RDC})\right)\right)^{-1} \int_0^t \exp(-(t-t')/\tau_r^{RDC}) R_k(\vec{r}^{\,N}(t'))dt', \tag{10}$$

and

$$\overline{P_k\left(\vec{r}^{\,N}(t)\right)}^{t,\exp} = \left(\tau_\theta^{RDC}\left(1-\exp(-t/\tau_\theta^{RDC})\right)\right)^{-1} \int_0^t \exp(-(t-t')/\tau_\theta^{RDC}) P_k(\vec{r}^{\,N}(t'))dt', \tag{11}$$

with τ_r^{RDC} and τ_θ^{RDC} their respective memory relaxation times. Generally, the memory relaxation times τ_r^{RDC} and τ_θ^{RDC} are chosen to be much longer than the MD or SD integration time step Δt,

$$\Delta t \ll \tau_r^{RDC} \ll \tau_\theta^{RDC} \ll t^{MD,SD} \quad , \tag{12}$$

where $t^{MD,SD}$ is the length of the MD or SD simulation.

2.3. Calculation of RDCs using rotational sampling and configurational averaging

Expressions for the RDC-restraining forces in the rotational-sampling (*MRS*) and configurational-averaging approach can be found in Ref.[23]. Dipolar couplings D_k were calculated using Eq. (2) during the simulations at every time step in order to obtain a high-resolution sampling $\langle D_k \rangle$ value when averaging in Eq. (6), while atomic coordinates were

stored at 2 ps intervals for post-simulation analysis. In the RDC-restraining simulations, the dipolar couplings D_k calculated at every time step were also used to obtain the exponentially damped time averages $\overline{P_k}^{t,\exp}$ and possibly $\overline{R_k}^{t,\exp}$, of Eqs. (10) and (11), which are used in the RDC-restraining potential-energy term. These exponentially damped RDC values will thus slightly differ from the ones calculated without exponential damping. In order to analyse all trajectories in the same way, when reporting RDC values, Eq. (6) is used.

2.4. Calculation of RDCs using the alignment-tensor approach

Using the alignment-tensor approach the alignment tensor or Saupe matrix[33]

$$S_{ij}(t) \equiv (3/2)\cos(\beta_i(t))\cos(\beta_j(t)) - (1/2)\delta_{ij} \qquad (i, j = 1, 2, 3) \qquad (13)$$

defines the orientation of the molecule relative to the direction of the magnetic field, that is, the magnetic field vector has angles $ß_1$, $ß_2$ and $ß_3$ with the *x*-, *y*- and *z*-axes, respectively, of a (right-handed) molecule-fixed coordinate system. δ_{ij} is the Kronecker delta. If the inter-nuclear vector $\vec{r}_{k_1k_2} \equiv \vec{r}_{k_1} - \vec{r}_{k_2}$ of a dipolar coupling $D_{k_1k_2}$ or in short D_k between two nuclear spins k_1 and k_2 has angles $\alpha_{k,1}$, $\alpha_{k,2}$ and $\alpha_{k,3}$ with the *x*-, *y*- and *z*-axes, respectively, of the (right-handed) molecule-fixed coordinate system, the dipolar coupling D_k can be expressed[10,17] in terms of the angles $\alpha_{k,i}$ and $ß_i$ (i = 1, 2, 3),

$$D_k(t) = D_k^c \sum_{i=1}^{3}\sum_{j=1}^{3} S_{ij}(t)\cos(\alpha_{k,i}(t))\cos(\alpha_{k,j}(t)), \qquad (14)$$

where it is assumed that $r_{k_1k_2}(t)$ is constant in time, $r_{k_1k_2}(t) = r_{k_1k_2}$. Eq. (14) involves two other assumptions: (*i*) All D_k or $\vec{r}_{k_1k_2}$ are related to the same alignment tensor S_{ij}, so have

a fixed alignment with respect to each other (the molecule is rigid); (*ii*) The direction of $\vec{r}_{k_1k_2}$ in the molecular coordinate system is independent of the alignment tensor, so the overall rotation of the molecule is decoupled from its internal motions.

Because the alignment tensor has only five independent components, Eq. (14) can be simplified[10,17] to

$$D_k(\vec{r}_{k_1k_2}(t); a_1(t), a_2(t), a_3(t), a_4(t), a_5(t)) = D_k^c \sum_{m=1}^{5} a_m(t) C_{k,m}(\vec{r}_{k_1k_2}(t)), \tag{15}$$

with

$$a_1(t) \equiv (3/2)(\cos(\beta_1(t))^2 - (1/2), \tag{16a}$$

$$a_2(t) \equiv (3/2)(\cos(\beta_2(t))^2 - (1/2), \tag{16b}$$

$$a_3(t) \equiv (3/2)\cos(\beta_1(t))\cos(\beta_2(t)), \tag{16c}$$

$$a_4(t) \equiv (3/2)\cos(\beta_1(t))\cos(\beta_3(t)), \tag{16d}$$

$$a_5(t) \equiv (3/2)\cos(\beta_2(t))\cos(\beta_3(t)), \tag{16e}$$

and

$$C_{k,1}(\vec{r}_{k_1k_2}(t)) \equiv (\cos(\alpha_{k,1}(t)))^2 - (\cos(\alpha_{k,3}(t)))^2, \tag{17a}$$

$$C_{k,2}(\vec{r}_{k_1k_2}(t)) \equiv (\cos(\alpha_{k,2}(t)))^2 - (\cos(\alpha_{k,3}(t)))^2, \tag{17b}$$

$$C_{k,3}(\vec{r}_{k_1k_2}(t)) \equiv 2\cos(\alpha_{k,1}(t))\cos(\alpha_{k,2}(t)), \tag{17c}$$

$$C_{k,4}(\vec{r}_{k_1k_2}(t)) \equiv 2\cos(\alpha_{k,1}(t))\cos(\alpha_{k,3}(t)), \tag{17d}$$

$$C_{k,5}(\vec{r}_{k_1k_2}(t)) \equiv 2\cos(\alpha_{k,2}(t))\cos(\alpha_{k,3}(t)). \tag{17e}$$

For each configuration of the molecule the values of the five coefficients a_m (m = 1, 2, 3, 4, 5) in Eq. (15) can be determined by minimising the difference between N_{RDC} target D_k^0

values or measured $D_k^{\exp}$ values and the calculated $D_k(\vec{r}_{k_1k_2};a_1,a_2,a_3,a_4,a_5)$ values as function of the a_m (m = 1, 2, 3, 4, 5). For example, one may minimise the function[10]

$$V^{AT}(\vec{r}_k,k=1,2,...,N_{RDC};a_1,a_2,a_3,a_4,a_5)\equiv$$

$$\sum_{k=1}^{N_{RDC}}(1/2)w_k^{RDC}(D_k(\vec{r}_{k_1k_2};a_1,a_2,a_3,a_4,a_5)/D_k^c-D_k^0/D_k^c)^2, \qquad (18)$$

with w_k^{RDC} the weight of RDC D_k in the minimisation. The values $a_m(t)$ (m = 1, 2, 3, 4, 5) that minimise expression Eq. (18) can be obtained from a system of five equations linear in $\underline{a}\equiv(a_1,a_2,a_3,a_4,a_5)^\tau$,

$$\underline{A}\underline{a}=\underline{g}, \qquad (19)$$

where the 5x5 matrix $\underline{A}$ has as elements (m,m' = 1, 2,…,5)

$$A_{m,m'}\equiv\sum_{k=1}^{N_{RDC}}w_k^{RDC}C_{k,m}(\vec{r}_{k_1k_2})C_{k,m'}(\vec{r}_{k_1k_2}), \qquad (20)$$

and the column matrix $\underline{g}\equiv(g_1,g_2,g_3,g_4,g_5)^\tau$ has as elements (m = 1, 2,…,5)

$$g_m\equiv\sum_{k=1}^{N_{RDC}}w_k^{RDC}(D_k^0/D_k^c)C_{k,m}(\vec{r}_{k_1k_2}). \qquad (21)$$

This system of five equations linear in a_m (m = 1, 2, 3, 4, 5) can be solved by standard techniques[34]. We note that in the alignment-tensor approach, by minimising Eq. (18) the values of D_k, which are of the order of kHz, will be scaled down towards the values of D_k^0, which are of the order of Hz. This is different from the rotational-sampling (*MRS*) approach, in which this reduction is obtained through rotational sampling.

In the alignment-tensor approach, the Cartesian coordinates $\vec{r}^{\,N}(t)$ and the magnetic field vector $\vec{H}(t)$ are specified with respect to a molecule-fixed (right-handed, Cartesian)

coordinate system, which has not yet been further defined. We may choose at each time step the space-fixed coordinate system as the molecule-fixed one, which choice avoids rotation of $\vec{r}^{\,N}(t)$ from the space-fixed coordinate system to the molecule-fixed one. By determining the quantities a_m (m = 1, 2, 3, 4, 5) at each time point t, the alignment is optimised per simulation step. Thus the a_m values will fluctuate in time, $a_m(t)$.

The values of the quantities $a_m(t)$ (m = 1, 2, 3, 4, 5), representing the alignment tensor, can be determined and used to calculate $D_k(t)$ values at every MD or SD time step (τ_{AT}^{RDC} =0). Alternatively, they can be, exponentially damped with memory relaxation time τ_{AT}^{RDC}, averaged over time yielding $\overline{a}_m^{t,\exp}$ values (m = 1, 2, 3, 4, 5)

$$\overline{a_m(t)}^{t,\exp} = \left(\tau_{AT}^{RDC}\left(1-\exp(-t/\tau_{AT}^{RDC})\right)\right)^{-1}\int_0^t \exp(-(t-t')/\tau_{AT}^{RDC})a_m(t')dt', \qquad (22)$$

or in terms of n discrete time steps Δt,

$$\overline{a_m(n\Delta t)}^{n\Delta t,\exp} = a_m(n\Delta t)\left(1-\exp(-\Delta t/\tau_{AT}^{RDC})\right)+\exp(-\Delta t/\tau_{AT}^{RDC})\overline{a_m((n-1)\Delta t)}^{(n-1)\Delta t,\exp}, \qquad (23)$$

and these averages used to calculate $D_k(t)$ at every MD or SD time step.

At every time step the $a_m(t)$ or $\overline{a}_m^{t,\exp}$ values are then used to calculate the dipolar couplings D_k using Eq. (15), which D_k values can be used in Eq. (8) to obtain exponentially damped average RDC values, to obtain the RDC-restraining forces, and also to obtain non-exponentially damped averaged RDC values. The quantities $a_m(t)$ (m = 1, 2, 3, 4, 5) determining the alignment-tensor were stored together with atomic coordinates at 2 ps intervals for post-simulation analysis.

3. Generating an anisotropic rotational distribution

In order to test the RDC restraining algorithms a simulation generating a non-isotropic rotational distribution should be performed. This can be achieved by introducing a biasing force in a simulation.

In an MD or SD simulation the angular distribution $P(\theta_{ab})$ of an axis '*ab*' in the molecule with respect to a hypothetical magnetic field direction $\vec{H}$, e.g. the z-direction, can be made (slightly) anisotropic by adding a biasing potential energy function[23] $V^{bias}\left(\theta_{bias}; K^{bias}, \theta^0_{bias}\right)$ to the potential energy function of the molecular system, that biases the distribution $P(\theta_{bias})$ toward a value θ^0_{bias}. The extent of the biasing is controlled by a strength parameter or force constant K^{bias}. Such a function V^{bias} should be continuous for all $\theta_{bias} \in [0,\pi]$ and have a continuous derivative with respect to θ_{bias} on this domain. In the current study the cosine-dependent biasing function of Ref.[23] was used with the axis '*ab*' defined by the two atoms with numbers 4 and 11 in Figure 1 as atoms *a* and *b*. θ-angle orientation-biasing *bSD* simulations[23] of length t^{SD} = 20 μs were performed using the biasing angle θ^0_{bias} = 0° and the biasing force constant K^{bias} = 0.2 kJ/mol, which led to $\langle D_k \rangle_t^{SD}$ values of the order of 10 Hz.

We note that the anisotropy introduced in $P(\theta_{abz})$ by a biasing potential energy term $V^{bias}\left(\theta_{abz}; K^{bias}, \theta^0_{bias}\right)$ will unlikely be the same as induced in an experiment.

4. Implementation, molecular model, simulation set-up and analysis

The simulations were performed using the GROMOS simulation software package[29,35-39].

4.1. Use of simple "toy" models or systems to optimise the testing of a method, model or algorithm

When methods are compared, their performance and range of applicability as function of the values of their parameters are to be evaluated. Use of a real molecular system, e.g. a protein for which measured RDC data are available, has some disadvantages:

1. The measured (RDC) data may be inconsistent with each other due to measurement errors. An example of such a situation for ^3J-couplings, which was detected using a simple "toy" model, can be found in Ref.[40].
2. Only a limited set of measured data or properties (observables) may be available, i.e. can be measured. This restricts the extent of testing in regard to varying the number and type of properties.
3. In contrast to a computational experiment, in a real experiment many quantities cannot be measured, in regard to RDCs for example, the non-uniform rotational distribution of the molecule, which leads to observable RDC values in the Hz range, is not experimentally measurable.
4. In a large molecule, such as a protein, many physical factors will determine the structure and dynamics of a molecule, for example its atomic composition, its covalent structure, its electrostatic interactions, its solvent or crystal

environment, etc. The presence of such factors may complicate a straightforward interpretation of an observed correlation between a parameter from the method or model and the measured data.

So, in order to optimise the comparison of methods or models, the (molecular) test system should be chosen as simple as possible without omitting features or degrees of freedom that are fundamental to the methods or models. In addition, the smaller the molecular test system, the less computational effort is required to evaluate the many combinations of parameter values of the methods or models to be compared.

4.2. Cyclo-octane with side-chain CH_2-CH_3 branches

As in Ref.[23], a cyclo-octane molecule with side-chain CH_2-CH_3 branches at all eight CH_1 united atoms of the ring was used as simple test system, see Figure 1. It allows for the use of 24 RDC bond vectors. It also allows for investigating the effect of the degree of intra-molecular flexibility on the calculated RDCs, while still being sufficiently small to thoroughly sample the rotational degrees of freedom of the molecule in an SD simulation in vacuo. In addition, the 24 bonds in the molecule are differently oriented, see Table 2 of Ref.[23], and thus will generate different $<D_k>$ values, depending on their angle θ_k with the z-axis, i.e. the direction of the magnetic field.

4.3. Interaction functions or force fields used

As in Ref.[23], the GROMOS 54A7 or 54B7 set (no difference for this cyclo-octane molecule) of force-field parameters (*GR*) was used[28]. The molecular topology file contains 16 CHn–CHn torsional dihedral-angle potential energy terms and seven improper dihedral-

angle energy terms at the chiral centres of the ring (atoms 3, 7, 10, 11, 15, 16, and 18 in Figure 1, see Supporting Information of Ref.[23]). The absence of an improper dihedral angle at the chiral centre atom 4 in the ring allows some flexibility of the ring. The length of the CHn-CHn bonds in this force field is 0.153 nm. Taking r^0 = 0.153 nm, $R_k(t)$, Eq. (4), equals 1. Using the gyromagnetic ratio of a ^{13}C atom (see Table 1 of Ref.[23]), the value of D_k^c, Eq. (3), becomes -4.243 kHz. In order to investigate the effect of molecular flexibility, SD simulations were performed, in which the torsional-angle potential-energy terms in the force field were omitted (*GRnt*).

Using the same force field (*ff*) in the biasing *bSD(ff)* simulations to generate RDC target values D_k^0 as in the RDC-restraining *rSD(ff)* simulations minimises its influence of the force field upon testing and comparing the RDC-restraining algorithm.

4.4. Simulation set-up

The molecule was simulated in vacuo using stochastic dynamics. The SD leap-frog algorithm[29,41] was used with a time step Δt = 2 fs, a reference temperature of 300 K, and using a friction coefficient[23] γ_i^{SD} = 0.24 ps^{-1}, which was taken the same for all united atoms. This friction coefficient optimises[23] the rotational sampling for the molecule. All bonds in the molecules were kept fixed using the SHAKE algorithm[42] with a relative geometric precision of 10^{-4}.

4.5. RDC restraining

The RDC restraining was performed using the three approaches described above (*MRS*;

AT: $\tau_{AT}^{RDC} = 0$;. $\tau_{AT}^{RDC} > 0$). Since the bonds in the molecules were kept fixed, no averaging of the RDC distances $r_{k_1k_2}$ was required. Only the RDC angles θ_k in Eq. (9) were subject to restraining. Applying molecular rotational sampling (*MRS*), the force constant K^{RDC} = 2 kJmol^{-1}Hz^{-2} and memory relaxation time τ_{θ}^{RDC} = 1 ns were used[23], and the flat-bottom range ΔD^0 = 1 Hz. Applying the alignment-tensor approach different values for the force constant K^{RDC} and the memory relaxation times τ_{D}^{RDC} and τ_{AT}^{RDC} were used, and the flat-bottom range ΔD^0 = 1 Hz. By using the target RDC values D_k^0 generated using a particular force field, for example the GROMOS force field 54B7 with (*GR*) or without (*GRnt*) torsional-angle energy terms, in both orientation-biasing simulations and RDC-restraining simulations, the effect of molecular flexibility upon the structures and their variation (flexibility) obtained by molecular rotational-sampling (*MRS*) or alignment-tensor (*AT*) RDC restraining can be investigated.

4.6. SD simulations performed

The following types of SD simulations were performed or are described elsewhere[23].

1. Two z-axis biased (and unrestrained) simulations using a biasing force dependent on the angle θ_{abz} of a vector $\vec{r}_{ab} = \vec{r}_a - \vec{r}_b$, defined by two atoms *a* and *b* in the molecule (Fig. 1), with the z-axis. The GROMOS force field 54B7 with and without torsional-angle energy terms was used. These simulations are indicated using the notation *bSD*. In order to obtain sufficient sampling of the overall rotation of the molecule, these simulations covered 20 μs[23].
2. Two RDC-restraining simulations using the molecular rotational-sampling and

configurational-averaging (*MRS*) method[23] (temperature about 280 K) and 220 RDC-restraining simulations using the alignment-tensor (*AT*) method (temperature about 280 K, except for a few cases, $\tau_D^{RDC} = 0$, $K^{RDC} \geq 0.05$ kJmol^{-1}Hz^{-2} and $\tau_{AT}^{RDC} \leq 10$ ps, where the molecular potential energy was much larger than in unrestrained simulations, see Table 2.). These simulations are indicated using the notation *MRS rSD* and *AT rSD*. The alignment-tensor approach was used in two ways, either the alignment tensor was determined at every SD time step ($\tau_{AT}^{RDC} = 0$) or its values were exponentially damped ($\tau_{AT}^{RDC} > 0$) during the simulation. The RDC-restraining simulations using the molecular rotational-sampling (*MRS*) algorithm are $t^{SD} = 20$ μs long[23]. The simulations applying the *AT* method are 20 ns long, much shorter because the rotation of the molecule need not be sampled and also with an eye to the large number of *AT* simulations to be performed in order to investigate the many possible *AT* parameter-value combinations.

4.7. Analysis of atomic trajectories and RDC values

Dipolar couplings D_k were calculated during the simulations at every time step in order to obtain a high-resolution sampling $\langle D_k \rangle$ value when averaging, while trajectory atomic coordinates were stored at 2 ps intervals for post-simulation analysis[39]. In order to analyse all trajectories in the same way, when reporting RDC values, exponential damping is not used.

The values of $\beta_i(t)$ (i = 1, 2, 3; i.e. x, y, z), which represent the orientation of the molecule relative to the direction of the magnetic field, can be calculated from inversion

of Eqs. (16),

$$\beta_1(t) = (1/2)\arccos\left(4a_1(t)/3\right), \tag{24a}$$

$$\beta_2(t) = (1/2)\arccos\left(4a_2(t)/3\right), \tag{24b}$$

$$\beta_3(t) = \arccos\left(2a_4(t)/(3\cos(\beta_1(t)))\right). \tag{24c}$$

The angle $\theta_{ab,H}$ between the vector $\vec{r}_{ab}$ connecting the atoms *a* and *b* in the molecule and the vector representing the direction of the magnetic field $\vec{H}$ can be obtained from

$$\theta_{ab,H}(t) = \arccos\left(\frac{x_{ab}(t)\cos(\beta_1(t)) + y_{ab}(t)\cos(\beta_2(t)) + z_{ab}(t)\cos(\beta_3(t))}{r_{ab}(t)}\right). \tag{25}$$

The non-uniformity of the β_i-distributions, or rather of the $\theta_{ab,H}$-distribution, obtained from the *AT* RDC-restraining simulations can be compared to the $\theta_{ab,H}$-distribution obtained from the *MRS* RDC-restraining simulations[23]. The $\theta_{ab,H}$ angle was calculated at every time step in order to obtain well converged $\theta_{ab,H}$-angle distributions. In some cases, the *AT* RDC-restraining simulations were extended beyond 30 ns in order to enhance the convergence of the $\theta_{ab,H}$-angle distributions.

5. Results and Discussion

The results are presented in 12 tables and 7 figures. Figure 1 shows the topology of the cyclo-octane molecule with eight aliphatic side chains and the atom sequence numbers. Tables 1 – 6 and Figures 2 – 6 show the results obtained for the relatively rigid version of the molecule using the standard GROMOS force field (*GR*), whereas Tables 7 – 12 and Figure 7 show the corresponding (to Tables 1 - 6 and Figure 6) results obtained for the relatively flexible version of the molecule using the GROMOS force field without any torsional-angle terms (*GRnt*). Tables 3 and 4 show results for τ_D^{RDC} = 0 ps and τ_D^{RDC} = 100 ps, respectively (*GR*), whereas Tables 9 and 10 show the corresponding results for the relatively flexible molecule (*GRnt*), respectively. Tables 5 and 6 use K^{RDC} = 0.01 kJmol^{-1}Hz^{-2}, τ_D^{RDC} = 0 ps, and K^{RDC} = 2 kJmol^{-1}Hz^{-2}, τ_D^{RDC} = 100 ps, respectively, for the relatively rigid molecule (*GR*), whereas Tables 11 and 12 use these parameter values for the relatively flexible molecule.

5.1. Recovering RDCs by RDC restraining

Table 1 offers an overview of the root-mean-square deviations (*RMSD*) of the RDC-values $< D_{k_1k_2} >_{t^{SD}}$ from their target values $D^0_{k_1k_2}$ averaged over the eight RDCs of the bonds in the ring, over the eight first side-chain bonds and over the eight second side-chain bonds in cyclo-octane. The *AT* RDC-restraining *rSD* simulations used 110 combinations of values of the RDC-restraining parameters τ_D^{RDC}, K^{RDC} and τ_{AT}^{RDC}. Table 2 shows the corresponding values of the average GROMOS force-field potential energy and RDC-

restraining energy. Tables 3 and 4 show the 24 individual $< D_{k_1k_2} >_{\tau^{SD}}$ values of cyclo-octane obtained from one molecular rotational-sampling (*MRS*) *rSD* simulation[23] as well as from *AT rSD* simulations for 18 combinations of values of the RDC-restraining parameters τ_D^{RDC}, K^{RDC} and τ_{AT}^{RDC}. The RDC-restraining was applied to all 24 bond vectors in cyclo-octane $\vec{r}_{k_1k_2}$ (k_1-k_2) (see Figure 1). Since the flat bottom of the RDC-restraining potential-energy well is $2\Delta D^0$ = 2 Hz wide, the $< D_{k_1k_2} >_{\tau^{SD}}$ values only get restrained when these deviate more than 1 Hz from the target $D^0_{k_1k_2}$ values. If the restraining forces cannot keep a particular $D^0_{k_1k_2}$ value within 2 Hz from its target value, we consider the deviation to be significant. In addition, the RDC-restraining energies should not become so large as to induce strain in the molecule, i.e. should not lead to significantly increased internal molecular energy.

The case $\tau_D^{RDC} = \tau_{AT}^{RDC} = 0$ ps represents the standard way molecular structure refinement of (bio-) molecules is carried out, i.e. without any averaging. Ignoring the molecular motion, which is limited for this small molecule though, standard RDC-restraining, based on varying the five alignment-tensor elements to bring the D_k-values as close as possible to the corresponding target D_k^0-values, is not able to reproduce the 24 D_k^0-values properly. Allowing for time-averaging of the 5 quantities a_m, determining the 5 alignment-tensor elements, $\tau_{AT}^{RDC} > 0$ ps, the D_k^0 target values are better approximated. Using the parameter values $\tau_D^{RDC} = 0$ ps, $K^{RDC} = 0.01$ kJmol^{-1}Hz^{-2} and $\tau_{AT}^{RDC} > 0$ ps reproduces the target D_k^0-values quite well in conjunction with a low restraining energy

E_{AT}^{RDC}, probably because of the fitting of D_k- values to D_k^0-values by varying the five elements of the alignment tensor at each SD step. Improved agreement between $< D_{k_1 k_2} >_{t^{SD}}$ and D_k^0 values is also observed when allowing for time-averaging of the dipolar couplings, τ_D^{RDC} > 0 ps. Lengthening the averaging time τ_D^{RDC}, the RDC-restraining force constant K^{RDC} may be increased, because the restraining force is proportional to K^{RDC}/τ_D^{RDC}. Considering τ_D^{RDC} > 0, the deviations from the target RDC-values range from 0.5 to 2.7 Hz, even when τ_{AT}^{RDC} = 0, but the restraining energies E_{AT}^{RDC} are, except for lower force-constant (K^{RDC}) values, non-negligible. Table 1 shows that the RDCs in the backbone (ring) are least easily reproduced, whereas the RDCs of the first side-chain bonds are most easily recovered.

Comparing the *AT* RDC-restraining *rSD* simulation results with those of the molecular rotational-sampling (*MRS*) algorithm[23], see Table 3 (τ_D^{RDC} = 0 ps) and Table 4 (τ_D^{RDC} = 100 ps), the picture is mixed. The *MRS* method, which involves no fitting of parameters, generally shows smaller *RMSD*($< D_k > - D_k^0$)-values than the *AT* method with τ_D^{RDC} = 0 ps and τ_{AT}^{RDC} = 0 ps (Table 3). Allowing time-averaging of the quantities a_m (m = 1, 2, …, 5) determining the five alignment-tensor elements, τ_{AT}^{RDC} > 0 ps, decreases the *RMSD* ($< D_k > - D_k^0$)-values to values comparable to those obtained by the *MRS* method, except for the first side-chain bonds which generally show low *AT RMSD*($< D_k > - D_k^0$)-values. A similar picture is obtained for τ_D^{RDC} = 100 ps (Table 4).

Figure 2 shows the time evolution of six RDCs (top to bottom: 2 backbone, 2 first side-

chain, 2 second side-chain bonds) in *AT rSD* simulations with τ_D^{RDC} = 0 ps, and τ_{AT}^{RDC} = 0, 10 and 100 ps (columns). For τ_{AT}^{RDC} = 0 ps changes in $< D_k >_t$ are still observed after 10 ns and the range of ±1 Hz around the target D_k^0-value is not reached in four cases. Allowing τ_{AT}^{RDC} > 0 ps improves convergence for the two second side-chain bonds. Using τ_D^{RDC} = 100 ps (Figure 3), the curves become smoother and the target values are better approximated for the two second side-chain bonds, but not for the two backbone bonds.

Figures 4 (τ_D^{RDC} = 0 ps) and 5 (τ_D^{RDC} = 100 ps) show the time evolution of the five quantities $a_m(t)$ (m = 1, 2,…5; rows) representing the alignment-tensor elements for τ_{AT}^{RDC} = 0 ps and 100 ps (columns). The values fluctuate considerably. Yet, the fluctuations seem rather similar for the 5 elements and the different cases.

The structural properties of the molecule, represented by averaged values of all 16 torsional angles in Tables 5 (τ_D^{RDC} = 0 ps) and 6 (τ_D^{RDC} = 100 ps), do not show significant differences between the different cases and also not between the *MRS* and *AT rSD* simulations. For τ_D^{RDC} = 0 ps and τ_{AT}^{RDC} = 0 ps, the largest deviations of the *AT* from the *MRS rSD* simulations are observed.

The atomic mobility, represented by the torsional-angle fluctuations in Tables 5 and 6, is generally comparable between the *AT rSD* simulations and the *MRS rSD* simulation. The relatively large RMSF values for the torsional angles *φ(7-3-4-5)*, *φ(5-4-18-16)* and *φ(3-4-5-6)* are due to the absence of an improper dihedral-angle force-field term at the chiral atom with sequence number 4 of the ring.

5.2. Recovering the orientation distribution by RDC restraining

Even if the target RDC-values are approximated well in an *MRS* or *AT rSD* simulation, the underlying rotational distribution of the molecule may not match the one that was used to generate the target RDC-values. An *MRS* (solid lines) and a few *AT rSD* $\theta_{ab,H}$-angle distributions are shown in Figure 6 (left panel: τ_D^{RDC} = 0 ps; right panel: τ_D^{RDC} = 100 ps), together with the orientation-biased *bSD* distribution (dot-dashed lines).

While the *MRS rSD* simulation reproduces the $\theta_{ab,H}$-angle distribution that was used to generate the target D_k^0-values quite well, this is not observed for the *AT rSD* simulations, irrespective of the τ_D^{RDC} or τ_{AT}^{RDC} values used. Figure 7 shows the same result for the more flexible molecule simulated with the GROMOS force field without torsional-angle terms (*GRnt*). This is not surprising, considering the procedure to determine the alignment-tensor elements. If good agreement between target and calculated RDC-values is obtained using the alignment-tensor approach, this apparently does not imply that these RDC-values are based on similar (between experiment and simulation) molecular rotational distributions.

5.3. Influence of molecular flexibility on RDC restraining

Tables 7 - 12 show the effect of enhanced flexibility of cyclo-octane on the orientation-biasing generated RDCs and the RDC-restraining towards these target RDC-values by using the GROMOS 54A7 force field but without any torsional-angle terms (*GRnt*) in the potential energy function in both the orientation-biasing (*bSD*) and the RDC-restraining (*rSD*) simulations.

Introducing flexibility in the force field (compare the D_k^0 target values obtained in

the *bSD* simulations with *GRnt* (Tables 9, 10) and *GR* (Tables 3, 4), the size of the D_k^0 target values gets slightly smaller for the backbone bonds, slightly larger for the first side-chain bonds. The only sizeable change in these 16 values is observed for bond 5-4, whose value switches from D_k^0 = -4.6 Hz using force field *GR* to D_k^0 = +6.2 Hz using the more flexible *GRnt* force field in the orientation-biasing simulations. This is due to the absence of an improper dihedral-angle force-field term at the chiral atom number 4 in the ring. Upon introducing flexibility into the force field, large changes in D_k^0 target values generated are observed for the second side-chain bonds. RDC values appear to be quite sensitive to the (local) flexibility of the molecule. A comparison of the values in Table 7 (*GRnt*) with the corresponding ones in Table 1 (*GR*) shows that introducing flexibility into the molecule leads to larger deviations from the RDC target values using the alignment-tensor method. Tables 9 and 10 show that for this more flexible molecule the *MRS* method yields better results than the *AT* method. This is not surprising considering the assumption of molecular rigidity inherent to the *AT* method.

Tables 11 and 12 show the average values of the 16 torsional angles of cyclo-octane and their root-mean-square fluctuations (RMSF) obtained when using the standard GROMOS 54A7 force field without any torsional-angle terms (*GRnt*) in the potential energy function in both, orientation-biasing (*bSD*) and RDC-restraining (*rSD*) simulations.

Introducing flexibility into the molecule (combination of *bSD* and *rSD* for *GRnt*, Tables 11, 12) leads to sizeable structural changes compared to using the standard GROMOS force field (combination of *bSD* and *rSD* for *GR*, Tables 5, 6). Torsional-angle

changes in the range [-30°,+59°] (*MRS*) are observed. As expected, without torsional-angle potential energy terms, the simulations generally show larger torsional-angle fluctuations, in particular for the backbone dihedral angles.

6. Conclusions

The structure determination or refinement of molecules based on residual dipolar couplings (RDCs) measured by NMR generally employs an alignment-tensor (*AT*) formalism. The values of the five elements of the alignment tensor, which represent a particular orientation distribution of the molecule with respect to the direction of the magnetic field applied and also the reduction of the size of the dipolar couplings (DCs) to RDCs from the kHz range to the Hz range of values, can be estimated either from the shape, moments of inertia, hydrodynamic shape or charge distribution of the molecule or by optimising the agreement between a sufficient number of calculated and target RDCs for a given set of RDCs. Use of an alignment tensor generally implies that the rotational motion of the molecule and its coupling to the internal motions is ignored. The extensions[20-22] of the *AT* formalism mentioned in the Introduction allow for a representation of small amplitude motion of parts of the molecule, but are not able to reflect the physical dynamics of the motion and they ignore the statistical-mechanical Boltzmann (energy-dependent) weights of the different molecular configurations. This means, as shown in the current study, that these extended *AT* approaches are expected to perform well for relatively rigid molecules, here represented by use of the standard GROMOS force field *GR*. These approaches also perform well when many structural restraints, i.e. NOE distance restraints, ^{3}J-coupling derived torsional-angle restraints and hydrogen-bond restraints are applied[21,22]. However, for flexible molecules, here represented by the use of the standard GROMOS force field without any torsional-angle energy terms (*GRnt*), in the absence of any other

restraints rigidifying the molecule, these methods do not perform well.

The effect of the two assumptions, i.e. no coupling between rotational and intra-molecular motions and rigidity of the molecule, have been investigated by comparison of the RDC-values and orientation distribution obtained from the *AT* structure determination approach with the corresponding values and orientation distribution obtained by applying a structural determination method[23] based on sampling the rotational and internal degrees of freedom of a molecule (*MRS*) explicitly. As test molecule a small, simple molecule, cyclo-octane with eight aliphatic side chains, was chosen. Using a standard molecular force field (*GR*) the molecule is relatively rigid, whereas using this force field without torsional-angle terms (*GRnt*) the molecule becomes more flexible. The values of the RDC-restraining force constant, K^{RDC}, of the memory relaxation time of the dipolar couplings, τ_D^{RDC}, and of the memory relaxation time of the five quantities a_m representing the alignment-tensor, τ_{AT}^{RDC}, were varied, the latter ones in order to investigate the effect of allowing a particular type of time-averaging ($\tau_D^{RDC} > 0$ ps, $\tau_{AT}^{RDC} > 0$ ps) in the calculations on the resulting orientation distribution and RDC-values.

The case $\tau_D^{RDC} = \tau_{AT}^{RDC} = 0$ ps represents the standard way molecular structure refinement of (bio-)molecules is carried out, i.e. without any time-averaging. Ignoring any molecular motion, which is limited for the relatively rigid molecule though, standard *AT* RDC-restraining is not able to reproduce the 24 D_k^0-values properly. Allowing for time-averaging either of the five quantities (a_m) representing the alignment tensor, $\tau_{AT}^{RDC} > 0$ ps,

or of the dipolar couplings, $\tau_D^{RDC} > 0$, the D_k^0 target values are better approximated. Yet, the non-uniformity of the orientation distribution, the $\theta_{ab,H}$-angle distribution that was used to generate the target D_k^0 -values, was not reproduced in the *AT rSD* simulations, irrespective of the τ_D^{RDC} or τ_{AT}^{RDC} values used. This is not surprising, considering the procedure to determine the alignment-tensor elements. Contributions from spherical harmonics of order different from 2, tensor ranks other than 2, do not play a role in the measurement of RDCs. This implies that using the *AT* formalism the orientation distribution of the molecule is likely to contain only components that are representable with spherical harmonics of order 2. In contrast, MD or SD simulation may generate a more general orientation distribution, which, as is shown here, can be reproduced using the molecular rotational-sampling *MRS* method for structure determination or refinement of molecules based on RDC data. Thus, even in the case the RDC target values are reproduced in *AT rSD* simulations, these values do not represent the underlying non-uniform rotational distribution of the molecule.

Considering the results for the more flexible molecule (*GRnt*), it is clear that the standard *AT* approach fails to reproduce the target RDC-values (see e.g. the data for the second side-chain bonds in Tables 9 and 10).

For the small molecule investigated, using either the more rigid force field (*GR*) or the more flexible one (*GRnt*), the average molecular structure obtained in the *AT rSD* simulations does not differ much from the one obtained using the molecular rotational and configurational sampling (*MRS*) approach. This is not very surprising in view of the

relatively rigid ring structure of the cyclo-octane molecule.

Summarising one may conclude that the assumptions of rigidity and independence of rotational and internal motions of a molecule restrict the applicability of the alignment-tensor approach to derive molecular structure from RDC data. For bio-molecules with flexible parts one would rather use a method that is based on sampling rotational and internal motions of a molecule, thereby staying closer to the experimental process leading to observable RDCs.

The application of the *MRS* method to proteins would require rather long simulation periods, which would, when including solvent molecules, require orders of magnitude more computing effort than currently available to the average bio-molecular modeler. In view of the continuingly increasing computing power, an order of magnitude every five years, application to proteins will become possible sooner or later. The past half century has known many examples of methods proposed while not yet applicable to large systems, that are now standardly used.

Data and Software Availability

The GROMOS software for biomolecular simulation is available at https://github.com/biomos under the GPL-2.0 license. The structure and topology of the cyclo-octane toy molecule is provided as a zip archive in the Supporting Information.

Supporting Information

Archive file with data in machine-readable format, including structure and topology files for the cyclo-octane toy model.

Table S1. Calculation of RDC-restraining forces using the alignment-tensor approach.

Acknowledgement

NH acknowledges funding by the Deutsche Forschungsgemeinschaft (DFG, German Research Foundation) under Germany's Excellence Strategy – EXC 2075 – 390740016.

References

(1) Clore, G. M.; Gronenborn, A. M. NMR structure determination of proteins and protein complexes larger than 20 kDa. *Curr. Opin. Chem. Biol.* **1998**, *2*, 564-570.

(2) Wüthrich, K. NMR studies of structure and function of biological macromolecules (Nobel Lecture). *J. Biomol. NMR* **2003**, *27*, 13-39.

(3) Dominguez, C.; Schubert, M.; Duss, O.; Ravindranathan, S.; Allain, F. H. T. Structure determination and dynamics of protein-RNA complexes by NMR spectroscopy. *Progr. NMR Spectr.* **2011**, *58*, 1-61.

(4) Schubert, M. Insights into Carbohydrate Recognition by 3D Structure Determination of Protein-Carbohydrate Complexes Using NMR. *Glycoscience Glycotechnology* **2017**, *10*, 101-122.

(5) Tolman, J. R.; Flanagan, J. M.; Kennedy, M. A.; Prestegard, J. H. Nuclear magnetic dipole interactions in field-oriented proteins: Information for structure determination in solution. *Proc. Natl. Acad. Sci. USA* **1995**, *92*, 9279-9283.

(6) Tjandra, N.; Bax, A. Direct measurement of distances and angles in biomolecules by NMR in dilute liquid crystalline medium. *Science* **1997**, *278*,1111-1114.

(7) Chen, K.; Tjandra, N. The Use of Residual Dipolar Coupling in Studying Proteins by NMR. *Top. Curr. Chem.* **2012**, *326*, 47-67.

(8) Harris, R. K.; Becker, E. D.; Cabral de Menezes, S. M.; Goodfellow, R.; Granger, P. NMR nomenclature: nuclear spin properties and conventions for chemical shifts. IUPAC Recommendations 2001. *Pure Appl. Chem.* **2001**, *73*, 1795-1818.

(9) Harris, R. K.; Becker, E. D.; Cabral de Menezes, S. M.; Goodfellow, R.; Granger, P. NMR

nomenclature: nuclear spin properties and conventions for chemical shifts. IUPAC Recommendations 2001. *Magn. Reson. Chem.* **2002**, *40*, 489-505.

(10) Wirz, L. N. Graph Theoretic and Electronic Properties of Fullerenes and Biasing Molecular Modelling Simulations with Experimental Residual Dipolar Couplings. *PhD thesis* **2015**, Massey University, Albany, New Zealand.

(11) Higman, V. A.; Boyd, J.; Smith, L. J.; Redfield, C. Residual Dipolar Couplings – Are multiple independent alignments always possible? *J. Biomol. NMR* **2011**, *49*, 53-60.

(12) Zweckstetter, M.; Bax, A. Prediction of sterically induced alignment in a dilute liquid crystalline phase: Aid to protein structure determination by NMR. *J. Am. Chem. Soc.* **2000**, *122*, 3791-3792.

(13) Azurmendi, H. F.; Bush, C. A. Tracking alignment from the moment of inertia tensor (TRAMITE) of biomolecules in neutral dilute liquid crystal solutions. *J. Am. Chem. Soc*. **2002**, *124*, 2426-2427.

(14) Wu, B.; Petersen, M.; Girard, F.; Tessari, M.; Wymenga, S. S. Prediction of molecular alignment of nucleic acids in aligned media. *J. Biomol. NMR* **2006**, *35*, 103-115.

(15) Almond, A.; Axelsen, J. B. Physical interpretation of residual dipolar couplings in neutral aligned media. *J. Am. Chem. Soc.* **2002**, *124*, 9986- 9987.

(16) Zweckstetter, M. NMR: prediction of molecular alignment from structure using the PALES software. *Nature Protocols* **2008**, *3*, 679-690.

(17) Wirz, L. N.; Allison, J. A. Fitting alignment tensor components to experimental RDCs, CSAs and RQCs. *J. Biomol. NMR* **2015**, *62*, 25-29.

(18) Sternberg, U,; Witter, R.; Ulrich, A. S. All-atom molecular dynamics simulations using orientational constraints from anisotropic NMR samples. *J. Biomol. NMR* **2007**, *38*, 23-39.

(19) Tzvetkova, P.; Sternberg, U.; Gloge, T.; Navarro-Vàzquez, A.; Luy, B. Configuration determination by residual dipolar couplings: accessing the full conformational space by molecular dynamics with tensorial constraints. *Chem. Sci.* **2019**, *10*, 8774-8791.

(20) Clore, G. M.; Gronenborn, A. M.; Bax, A. A Robust Method for Determining the Magnitude of the Fully Asymmetric Alignment Tensor of Oriented Macromolecules in the Absence of Structural Information. *J. Magn. Res.* **1998**, *133*, 216-221.

(21) Clore, G. M.; Schwieters, C. D. How Much Backbone Motion in Ubiquitin is Required to Account for Dipolar Coupling Data Measured in Multiple Alignment Media as Assessed by Independent Cross-Validation ? *J. Am. Chem. Soc.* **2004**, *126*, 2923-2938.

(22) Lorieau, J. L.; Louis, J. M.; Schwieters, C. D.; Bax, A. pH triggered, activated-state conformations of the influenza hemagglutinin fusion peptide revealed by NMR. *Proc. Nat. Acad. Sci. USA*, **2012**, *109*, 19994-19999.

(23) van Gunsteren, W. F.; Pechlaner, M.; Smith, L. J.; Stankiewicz, B.; Hansen, N. A Method to Derive Structural Information on Molecules from Residual Dipolar Coupling NMR data. *J. Phys. Chem.* **2022**, *126*, 3867-3888.

(24) van Gunsteren, W. F.; Allison, J. A.; Daura, X.; Dolenc, J.; Hansen, N.; Mark, A. E.; Oostenbrink, C.; Rusu, V. H.; Smith, L. J. Deriving Structural Information from Experimentally Measured Data on Biomolecules. *Angew. Chem. Int. Ed.* **2016**, *55***,** 15990-16010.

(25) van Gunsteren, W. F.; Berendsen, H. J. C., Groningen Molecular Simulation (GROMOS)

Library Manual; BIOMOS b.v., University of Groningen, Groningen, 1987.

(26) van Gunsteren, W. F.; Billeter, S. R.; Eising, A. A.; Hünenberger, P. H.; Krüger, P.; Mark, A. E.; Scott, W. R. P.; Tironi, I. G. Biomolecular Simulation: The GROMOS96 Manual and User Guide, Vdf Hochschulverlag AG an der ETH Zürich, Zürich, Switzerland, **1996**, 1-1042, ISBN 3 7281 2422 2.

(27) Oostenbrink, C.; Villa, A.; Mark, A. E.; van Gunsteren, W. F. A biomolecular force field based on the free enthalpy of hydration and solvation: the GROMOS force-field parameter sets 53A5 and 53A6. *J. Comput. Chem.* **2004**, *25*, 1656–76.

(28) Schmid, N.; Eichenberger, A. P.; Choutko, A.; Riniker, S.; Winger, M.; Mark, A. E.; van Gunsteren, W. F. Definition and testing of the GROMOS force-field versions 54A7 and 54B7. *Eur. Biophys. J.* **2011**, *40*, 843−856.

(29) van Gunsteren, W. F., Christ, C. D.; Christen, M.; Eichenberger, A. P., Hansen, N.; Hünenberger, P. H.; Oostenbrink, C.; Pechlaner, M.; Riniker, S.; Schmid, N. The GROMOS Software for (Bio)Molecular Simulation. Volumes 1 – 9. **2024** http://www.gromos.net/. Accessed 4 January 2024.

(30) van Gunsteren, W. F.; Boelens, R.; Kaptein, R.; Scheek, R. M.; Zuiderweg, E. R. P. An Improved Restrained Molecular Dynamics Technique to Obtain Protein Tertiary Structure from Nuclear Magnetic Resonance Data. In: "Molecular Dynamics and Protein Structure", J. Hermans ed., Polycrystal Book Service, P.O. Box 27, Western Springs, Ill. 60558, USA, **1985**, 92-99.

(31) Torda, A. E.; Scheek, R. M.; van Gunsteren, W. F. Time-dependent distance restraints in molecular dynamics simulations. *Chem. Phys. Letters* **1989**, *157*, 289-294.

(32) Torda, A. E.; Scheek, R. M.; van Gunsteren, W. F. Time-averaged Nuclear Overhauser Effect Distance Restraints Applied to Tendamistat. *J. Mol. Biol.* **1990**, *214*, 223-235.

(33) Saupe, A. Kernresonanzen in kristallinen Flüssigkeiten und in kristallinflüssigen Lösungen. *Zeitung für Naturforschung* **1964**, *19a*, 161-171.

(34) Press, W. H. ; Teukolsky, S. A. ; Vetterling, W. T. ; Flannery, B. P. Numerical Recipies in C. the Art of Scientific Computing, 2nd Edition, Cambridge University Press, Cambridge, U.K., (**1967**).

(35) Schmid, N.; Christ, C. D.; Christen, M.; Eichenberger, A. P., van Gunsteren, W. F. Architecture, implementation and parallelization of the GROMOS software for biomolecular simulation. *Comp. Phys. Comm.* **2012**, *183*, 890-903.

(36) Kunz, A. P. E.; Allison, J. R.; Geerke, D. P.; Horta, B. A. C.; Hünenberger, P. H.; Riniker, S.; Schmid, N.; van Gunsteren, W. F. New functionalities in the GROMOS biomolecular simulation software. *J. Comput. Chem.* **2012**, *33*, 340-353.

(37) Schmid, N.; Allison, J. R.; Dolenc, J.; Eichenberger, A. P.; Kunz, A. P. E.; van Gunsteren, W. F. Biomolecular structure refinement using the GROMOS simulation software. *J. Biomolecular NMR* **2011**, *51*, 265-281.

(38) Riniker, S.; Christ, C. D.; Hansen, H. S.; Hünenberger, P. H.; Oostenbrink, C.; Steiner, D.; van Gunsteren, W. F. Calculation of relative free energies for ligand-protein binding, solvation and conformational transitions using the GROMOS software. *J. Phys. Chem.* **2011**, *B 115*, 13570-13577.

(39) Eichenberger, A. P.; Allison, J. R.; Dolenc, J.; Geerke, D. P.; Horta, B. A. C.; Meier, K.; Oostenbrink, C.; Schmid, N.; Steiner, D.; Wang, D.; van Gunsteren, W. F. GROMOS++ software

for the analysis of biomolecular simulation trajectories. *J. Chem. Theory. Comp.* **2011**, *7*, 3379-3390.

(40) Allison, J. R.; van Gunsteren, W. F. A method to explore protein side chain conformational variability using experimental data. *ChemPhysChem* **2009,** *10*, 3213-3228.

(41) van Gunsteren, W. F.; Berendsen, H. J. C. A leap-frog algorithm for stochastic dynamics. *Molec. Simul.* **1988**, *1*, 173-185.

(42) Ryckaert, J. P.; Ciccotti, G.; Berendsen, H. J. C. Numerical integration of the Cartesian equations of motion of a system with constraints: Molecular dynamics of n-alkanes. *J. Comput. Phys.* **1977**, *23*, 327–341.

Tables

Table 1. Root-mean-square deviations (*RMSD*) of the RDC-values $< D_{k_1k_2} >_{t^{SD}}$ from their target values $D^0_{k_1k_2}$ averaged over the eight RDCs of the bonds in the ring, the first side-chain bonds and the second side-chain bonds in cyclo-octane. The $< D_{k_1k_2} >_{t^{SD}}$ values (Hz) were calculated from 24 bond-vector RDC-restraining t^{SD} = 30 ns *AT rSD* simulations with γ^{SD} = 0.24 ps^{-1} for all 24 bond vectors $\vec{r}_{k_1k_2}$ (***k*₁-*k*₂**), see Figure 1. The *AT* RDC-restraining function parameter values K^{RDC}, τ_D^{RDC} and τ_{AT}^{RDC} are varied, ΔD^0 = 1 Hz. The $D^0_{k_1k_2}$ target values for the 24 bond vectors were obtained from orientation-biasing *bSD* simulations[23] with γ^{SD} = 0.24 ps^{-1} and t^{SD} = 20 μs using the orientation-biasing function parameter values K^{bias} = 0.2 kJmol^{-1} and θ^0_{bias} = 0°. In all simulations the GROMOS force field (***GR***) was used. *RMSD* values larger than 2 Hz are in italics. "-": Result not available due to SHAKE failure: too large forces.

τ_D^{RDC} (ps)	K^{RDC} (kJmol^{-1} Hz^{-2})	*RMSD* ($< D_{k_1k_2} >_{t^{SD}}$ - $D^0_{k_1k_2}$) (Hz)														
		Backbone bonds					First side-chain bonds					Second side-chain bonds				
		AT: τ_{AT}^{RDC} (ps)					*AT:* τ_{AT}^{RDC} (ps)					*AT:* τ_{AT}^{RDC} (ps)				
		0	1	10	10^2	10^3	0	1	10	10^2	10^3	0	1	10	10^2	10^3
0	0.01	*2.5*	2.0	1.0	1.0	*2.3*	0.8	0.5	0.5	0.6	0.8	*2.3*	1.2	1.0	1.1	1.8
	0.02	*4.0*	*2.4*	2.0	1.9	2.0	*2.4*	0.6	0.5	0.6	0.5	*5.7*	*2.2*	1.2	1.0	1.1
	0.05	*5.9*	*2.8*	*2.6*	*2.1*	1.8	*4.4*	0.7	0.9	0.6	0.6	*9.9*	*3.5*	*2.5*	1.4	1.2
	0.1	*6.3*	*3.8*	*3.5*	*2.2*	*2.1*	*5.3*	1.8	2.0	0.6	0.6	*11.0*	*5.7*	*4.7*	1.6	1.4
	0.2	*6.4*	*4.3*	*4.1*	*2.5*	2.0	*5.2*	1.9	*2.4*	0.8	0.6	*11.1*	*6.8*	*6.2*	*2.2*	1.2
	0.5	-	*4.5*	*4.8*	*3.3*	-	-	*2.8*	*3.7*	1.6	-	-	*7.4*	*8.1*	*4.1*	-
1	0.2	2.0	*2.7*	*2.2*	*2.1*	1.9	0.5	1.5	0.6	0.6	0.6	1.2	*2.7*	1.5	1.5	1.0
	0.5	*2.5*	1.9	*2.2*	*2.1*	*2.0*	0.9	0.6	0.7	0.6	0.6	*2.1*	1.2	1.6	1.4	1.2

	1.0	*2.6*	*2.1*	2.0	*2.2*	*2.1*	1.3	0.6	0.5	0.6	0.6	*2.6*	1.4	1.1	1.5	1.3
10	0.2	2.0	*2.1*	*2.1*	1.9	*2.1*	0.6	0.6	0.6	0.6	0.6	1.1	1.3	1.3	1.0	1.4
	0.5	1.9	*2.1*	*2.1*	*2.1*	*2.1*	0.6	0.6	0.6	0.6	0.6	1.1	1.4	1.5	1.3	1.3
	1	1.9	2.0	1.9	2.0	1.9	0.6	0.5	0.6	0.6	0.5	1.0	1.2	1.1	1.2	1.1
100	0.2	*2.4*	2.0	2.0	2.0	1.9	0.8	0.6	0.5	0.6	0.6	1.9	1.2	1.2	1.2	1.0
	0.5	*2.1*	*2.2*	2.0	2.0	*2.1*	0.6	0.6	0.6	0.5	0.6	1.3	1.5	1.3	1.2	1.3
	1	*2.1*	1.9	1.8	*2.4*	1.9	0.6	0.6	0.6	0.8	0.6	1.3	1.1	1.0	2.0	1.1
	2	2.0	2.0	2.0	*2.1*	*2.1*	0.7	0.5	0.6	0.6	0.6	1.2	1.2	1.2	1.3	1.3
	5	1.9	2.0	1.9	1.9	1.9	0.6	0.6	0.6	0.6	0.6	1.1	1.3	1.0	1.0	1.0
1000	1	1.9	*2.5*	*2.2*	1.8	2.0	0.6	1.1	0.7	0.6	0.5	1.0	*2.3*	1.6	0.9	1.2
	2	1.8	2.0	*2.3*	*2.2*	2.0	0.6	0.6	0.7	0.7	0.5	1.0	1.2	1.7	1.5	1.2
	5	1.8	*2.2*	2.0	1.9	2.0	0.6	0.6	0.6	0.6	0.6	1.0	1.5	1.3	1.1	1.2
	10	2.0	2.0	1.9	1.9	1.8	0.6	0.6	0.6	0.6	0.6	1.3	1.2	1.0	1.0	0.9
	100	1.9	1.9	*2.1*	*2.2*	1.9	0.6	0.6	0.6	0.7	0.6	1.1	1.0	1.4	1.6	1.1

Table 2. Average GROMOS force-field potential energy E_{pot} and RDC-restraining energy E_{AT}^{RDC} in cyclo-octane calculated from 24 bond-vector RDC-restraining *AT rSD* simulations of length t^{SD} = 30 ns with γ^{SD} = 0.24 ps^{-1} for all 24 bond vectors $\vec{r}_{k_1k_2}$ (***k*₁-*k*₂**), see Figure 1. The *AT* RDC-restraining function parameter values K^{RDC}, τ_D^{RDC} and τ_{AT}^{RDC} are varied, ΔD^0 = 1 Hz. The $D^0_{k_1k_2}$ target values for the 24 bond vectors were obtained from orientation-biasing *bSD* simulations[23] with γ^{SD} = 0.24 ps^{-1} and t^{SD} = 20 μs using the orientation-biasing function parameter values K^{bias} = 0.2 kJmol^{-1} and θ^0_{bias} = 0°. In all simulations the GROMOS force field (***GR***) was used. "-": Result not available due to SHAKE failure: too large forces.

τ_D^{RDC} (ps)	K^{RDC} (kJmol^{-1} Hz^{-2})	Potential energy (kJ/mol)									
		GROMOS molecular energy E_{pot}					RDC-restraining energy E_{AT}^{RDC}				
		AT: τ_{AT}^{RDC} (ps)					*AT:* τ_{AT}^{RDC} (ps)				
		0	1	10	10^2	10^3	0	1	10	10^2	10^3
0	0.01	96	95	94	94	95	2	1	1	1	2
	0.02	99	96	94	94	94	7	3	2	2	2
	0.05	106	100	96	95	94	30	11	9	6	4
	0.1	126	107	100	94	94	70	33	30	13	12
	0.2	230	121	105	97	94	147	76	74	34	22
	0.5	-	188	119	101	-	-	221	210	134	-
1	0.2	94	97	94	94	94	10	30	14	14	6
	0.5	95	95	94	94	94	54	22	38	31	23
	1.0	96	95	94	94	94	143	66	44	71	57
10	0.2	94	95	94	94	94	5	8	8	3	8
	0.5	94	94	94	95	94	11	21	24	21	18

	1	94	94	94	94	94	19	30	20	26	26
100	0.2	95	94	94	94	94	13	5	5	5	2
	0.5	94	95	94	94	94	16	23	14	11	14
	1	95	94	94	95	94	30	16	6	66	16
	2	94	94	94	94	94	61	53	49	60	52
	5	94	94	94	94	94	62	138	58	52	41
1000	1	94	96	94	93	94	4	48	30	3	8
	2	94	94	94	95	94	6	21	56	44	15
	5	94	94	94	94	94	19	131	58	24	40
	10	94	94	94	94	94	135	117	37	51	28
	100	94	94	94	95	94	560	324	1008	3669	507

Table 3. RDC $< D_{k_1k_2} >_{t^{SD}}$ values (Hz) obtained for cyclo-octane as calculated from 24 bond-vector RDC-restraining *rSD* simulations with γ^{SD} = 0.24 ps^{-1} for all 24 bond vectors $\vec{r}_{k_1k_2}$(***k*₁-*k*₂**), see Figure 1. *RMSD*: root-mean-square difference between $< D_{k_1k_2} >_{t^{SD}}$ and $D^0_{k_1k_2}$ for the eight bond-vector RDCs. The molecular rotational-sampling (*MRS*) simulation[23] is t^{SD} = 20 μs long, while the alignment-tensor (*AT*) simulations are t^{SD} = 30 ns long. The *MRS* RDC-restraining function parameter values are K^{RDC} = 2 kJmol^{-1}Hz^{-2}, τ_θ^{RDC} = 1 ns, and ΔD^0 = 1 Hz. The *AT* RDC-restraining function parameter values K^{RDC} and τ_{AT}^{RDC} are varied and τ_D^{RDC} = **0 ps**, ΔD^0 = 1 Hz. The sequence numbers of the atoms are given in Figure 1. The $D^0_{k_1k_2}$ target values for the 24 bond vectors were obtained from orientation-biasing *bSD* simulations[23] with γ^{SD} = 0.24 ps^{-1} and t^{SD} = 20 μs using the orientation-biasing function parameter values K^{bias} = 0.2 kJmol^{-1} and θ^0_{bias} = 0°. In all simulations the GROMOS force field (***GR***) was used. Deviations of averaged RDC-values $< D_{k_1k_2} >_{t^{SD}}$ from their target values $D^0_{k_1k_2}$ larger than 2 Hz are in italics.

AT: K^{RDC} (kJmol^{-1} Hz^{-2})	Backbone bonds						First side-chain bonds						Second side-chain bonds					
	Bond vector $\vec{r}_{k_1k_2}$	$D^0_{k_1k_2}$ (Hz)	$< D_{k_1k_2} >_{t^{SD}}$ (Hz)				Bond vector $\vec{r}_{k_1k_2}$	$D^0_{k_1k_2}$ (Hz)	$< D_{k_1k_2} >_{t^{SD}}$ (Hz)				Bond vector $\vec{r}_{k_1k_2}$	$D^0_{k_1k_2}$ (Hz)	$< D_{k_1k_2} >_{t^{SD}}$ (Hz)			
			MRS	*AT:* τ_{AT}^{RDC} (ps)					*MRS*	*AT:* τ_{AT}^{RDC} (ps)					*MRS*	*AT:* τ_{AT}^{RDC} (ps)		
			-	0	10	100			-	0	10	100			-	0	10	100
0.01	**3-4**	-6.7	-5.9	*-4.5*	-5.0	-5.0	**2-3**	-7.5	-6.3	-7.6	-7.3	-7.3	**1-2**	13.8	12.3	*10.2*	13.2	13.2
	4-18	-7.5	-6.4	*-5.0*	-5.8	-5.8	**5-4**	-4.6	-3.9	-3.2	-5.2	-5.1	**6-5**	11.6	10.4	*9.0*	11.0	10.8
	18-16	15.7	*13.1*	*12.8*	*13.4*	*13.4*	**19-18**	-7.4	-6.4	-7.0	-7.0	-6.9	**20-19**	15.6	13.7	*12.0*	14.7	14.6

	16-15	16.2	*13.5*	*13.6*	*14.1*	*14.1*	**17-16**	-10.1	-8.5	-9.6	-9.4	-9.4	**23-17**	-2.9	-3.1	-1.9	-2.1	-2.1
	15-11	-6.7	-6.1	*-4.2*	-4.9	-4.9	**21-15**	-7.2	-6.0	-6.5	-6.7	-6.6	**22-21**	-5.8	-5.0	-4.9	-4.7	-4.6
	11-10	-7.0	-5.9	-4.9	-5.5	-5.5	**13-11**	-3.9	-3.4	-4.3	-4.2	-4.2	**14-13**	13.8	*11.6*	*11.6*	12.1	12.1
	10-7	15.6	*13.2*	*13.0*	*13.5*	*13.4*	**12-10**	-6.8	-5.5	-6.7	-6.5	-6.5	**24-12**	-6.2	-5.9	-4.8	-5.0	-4.9
	7-3	16.1	*13.2*	*13.5*	*14.0*	*14.0*	**8-7**	-10.6	-9.2	-9.4	-9.7	-9.6	**9-8**	-3.5	-3.0	-2.4	-2.7	-2.7
	RMSD		2.0	*2.5*	1.9	1.9	*RMSD*		1.2	0.8	0.5	0.6	*RMSD*		1.3	*2.3*	1.0	1.1
0.05	**3-4**	-6.7	-5.9	*-1.9*	-4.5	-5.0	**2-3**	-7.5	-6.3	-7.8	-7.5	-7.2	**1-2**	13.8	12.3	*-2.1*	*10.0*	12.5
	4-18	-7.5	-6.4	*-1.6*	*-5.0*	-5.7	**5-4**	-4.6	-3.9	*7.3*	-2.6	-4.4	**6-5**	11.6	10.4	*-2.1*	*8.6*	10.3
	18-16	15.7	*13.1*	*8.8*	*12.6*	*13.2*	**19-18**	-7.4	-6.4	-5.9	-6.8	-6.9	**20-19**	15.6	13.7	*-0.9*	*11.6*	13.8
	16-15	16.2	*13.5*	*9.8*	*13.4*	*13.9*	**17-16**	-10.1	-8.5	-9.4	-9.4	-9.3	**23-17**	-2.9	-3.1	*-0.4*	-1.9	-2.0
	15-11	-6.7	-6.1	*-0.5*	*-4.2*	-4.9	**21-15**	-7.2	-6.0	-5.2	-6.4	-6.5	**22-21**	-5.8	-5.0	*-2.4*	-4.5	-4.6
	11-10	-7.0	-5.9	*-2.3*	*-4.9*	-5.4	**13-11**	-3.9	-3.4	-3.7	-4.2	-4.2	**14-13**	13.8	*11.6*	*8.4*	*11.5*	11.9
	10-7	15.6	*13.2*	*9.5*	*12.8*	*13.3*	**12-10**	-6.8	-5.5	-7.2	-6.6	-6.2	**24-12**	-6.2	-5.9	*-2.1*	-4.5	-4.9
	7-3	16.1	*13.2*	*10.1*	*13.3*	*13.7*	**8-7**	-10.6	-9.2	*-7.3*	-9.2	-9.5	**9-8**	-3.5	-3.0	*-0.5*	-2.3	-2.7
	RMSD		2.0	*5.9*	*2.6*	*2.1*	*RMSD*		1.2	*4.4*	0.9	0.6	*RMSD*		1.3	*9.9*	*2.5*	1.4
0.1	**3-4**	-6.7	-5.9	*-2.1*	*-3.9*	-4.8	**2-3**	-7.5	-6.3	-6.3	-7.6	-7.4	**1-2**	13.8	12.3	*-3.0*	*6.3*	12.0
	4-18	-7.5	-6.4	*-2.0*	*-4.0*	*-5.4*	**5-4**	-4.6	-3.9	*8.6*	*0.6*	-4.1	**6-5**	11.6	10.4	*-3.9*	*5.8*	9.9
	18-16	15.7	*13.1*	*7.8*	*11.5*	*13.1*	**19-18**	-7.4	-6.4	*-5.0*	-6.7	-6.8	**20-19**	15.6	13.7	*-2.4*	*7.7*	*13.5*
	16-15	16.2	*13.5*	*8.8*	*12.4*	*13.8*	**17-16**	-10.1	-8.5	*-7.6*	-9.4	-9.5	**23-17**	-2.9	-3.1	-1.0	-1.5	-1.9
	15-11	-6.7	-6.1	*-1.3*	*-3.3*	*-4.6*	**21-15**	-7.2	-6.0	*-4.1*	-5.9	-6.5	**22-21**	-5.8	-5.0	*-2.6*	-3.9	-4.4
	11-10	-7.0	-5.9	*-2.3*	*-4.2*	-5.3	**13-11**	-3.9	-3.4	-2.1	-4.1	-4.2	**14-13**	13.8	*11.6*	*4.8*	*10.7*	11.9
	10-7	15.6	*13.2*	*8.7*	*12.0*	*13.2*	**12-10**	-6.8	-5.5	-5.3	-6.6	-6.6	**24-12**	-6.2	-5.9	*-2.4*	*-3.9*	-4.7
	7-3	16.1	*13.2*	*8.5*	*12.3*	*13.7*	**8-7**	-10.6	-9.2	*-6.2*	-8.6	-9.4	**9-8**	-3.5	-3.0	*-1.3*	-1.8	-2.5
	RMSD		2.0	*6.3*	*3.5*	*2.2*	*RMSD*		1.2	*5.3*	2.0	0.6	*RMSD*		1.3	*11.0*	*4.7*	1.6
0.2	**3-4**	-6.7	-5.9	*-2.7*	*-3.2*	*-4.6*	**2-3**	-7.5	-6.3	*-4.6*	-8.0	-7.4	**1-2**	13.8	12.3	*-2.3*	*3.4*	*10.8*
	4-18	-7.5	-6.4	*-2.8*	*-3.0*	*-5.1*	**5-4**	-4.6	-3.9	*5.9*	*1.6*	-3.2	**6-5**	11.6	10.4	*-1.9*	*4.9*	*9.0*

	18-16	15.7	*13.1*	*7.6*	*11.1*	*12.8*	**19-18**	-7.4	-6.4	*-4.1*	-6.7	-6.8	**20-19**	15.6	13.7	*-2.2*	*4.8*	*12.3*
	16-15	16.2	*13.5*	*8.2*	*11.8*	*13.5*	**17-16**	-10.1	-8.5	*-6.1*	-9.9	-9.5	**23-17**	-2.9	-3.1	-1.9	-1.2	-1.8
	15-11	-6.7	-6.1	*-2.4*	*-2.3*	*-4.3*	**21-15**	-7.2	-6.0	*-3.4*	-6.0	-6.3	**22-21**	-5.8	-5.0	*-2.4*	*-3.2*	-4.2
	11-10	-7.0	-5.9	*-2.7*	*-3.4*	-5.0	**13-11**	-3.9	-3.4	*0.3*	-4.1	-4.1	**14-13**	13.8	*11.6*	*0.0*	*10.1*	*11.7*
	10-7	15.6	*13.2*	*8.2*	*11.6*	*12.9*	**12-10**	-6.8	-5.5	*-3.6*	-7.2	-6.7	**24-12**	-6.2	-5.9	*-2.5*	*-3.2*	-4.4
	7-3	16.1	*13.2*	*7.8*	*11.9*	*13.5*	**8-7**	-10.6	-9.2	*-5.6*	-8.6	-9.3	**9-8**	-3.5	-3.0	-2.0	*-1.2*	-2.3
	RMSD		2.0	*6.4*	*4.1*	*2.5*	*RMSD*		1.2	*5.2*	*2.4*	0.8	*RMSD*		1.3	*11.1*	*6.2*	*2.2*

Table 4. RDC $< D_{k_1k_2} >_{t^{SD}}$ values (Hz) obtained for cyclo-octane as calculated from 24 bond-vector RDC-restraining *rSD* simulations with γ^{SD} = 0.24 ps^{-1} for all 24 bond vectors $\vec{r}_{k_1k_2}$(***k₁-k₂***), see Figure 1. *RMSD*: root-mean-square difference between $< D_{k_1k_2} >_{t^{SD}}$ and $D^0_{k_1k_2}$ for the eight bond-vector RDCs. The molecular rotational-sampling (*MRS*) simulation[23] is t^{SD} = 20 μs long, while the alignment-tensor (*AT*) simulations are t^{SD} = 30 ns long. The *MRS* RDC-restraining function parameter values are K^{RDC} = 2 kJmol^{-1}Hz^{-2}, τ_θ^{RDC} = 1 ns, and ΔD^0 = 1 Hz. The *AT* RDC-restraining function parameter values K^{RDC} and τ_{AT}^{RDC} are varied and τ_D^{RDC} = **100 ps**, ΔD^0 = 1 Hz. The sequence numbers of the atoms are given in Figure 1. The $D^0_{k_1k_2}$ target values for the 24 bond vectors were obtained from orientation-biasing *bSD* simulations[23] with γ^{SD} = 0.24 ps^{-1} and t^{SD} = 20 μs using the orientation-biasing function parameter values K^{bias} = 0.2 kJmol^{-1} and θ^0_{bias} = 0°. In all simulations the GROMOS force field (***GR***) was used. Deviations of averaged RDC-values $< D_{k_1k_2} >_{t^{SD}}$ from their target values $D^0_{k_1k_2}$ larger than 2 Hz are in italics.

AT: K^{RDC} (kJmol^{-1} Hz^{-2})	Backbone bonds						First side-chain bonds						Second side-chain bonds					
	Bond vector $\vec{r}_{k_1k_2}$	$D^0_{k_1k_2}$ (Hz)	$< D_{k_1k_2} >_{t^{SD}}$ (Hz)				Bond vector $\vec{r}_{k_1k_2}$	$D^0_{k_1k_2}$ (Hz)	$< D_{k_1k_2} >_{t^{SD}}$ (Hz)				Bond vector $\vec{r}_{k_1k_2}$	$D^0_{k_1k_2}$ (Hz)	$< D_{k_1k_2} >_{t^{SD}}$ (Hz)			
			MRS	*AT:* τ_{AT}^{RDC} (ps)					*MRS*	*AT:* τ_{AT}^{RDC} (ps)					*MRS*	*AT:* τ_{AT}^{RDC} (ps)		
			-	0	10	100			-	0	10	100			-	0	10	100
1	**3-4**	-6.7	-5.9	-5.0	-5.1	-4.7	**2-3**	-7.5	-6.3	-7.4	-7.3	-7.4	**1-2**	13.8	12.3	12.5	13.5	*11.4*
	4-18	-7.5	-6.4	-5.7	-5.9	*-5.2*	**5-4**	-4.6	-3.9	-4.5	-5.5	-3.2	**6-5**	11.6	10.4	10.4	11.2	*9.0*
	18-16	15.7	*13.1*	*13.2*	*13.5*	*12.8*	**19-18**	-7.4	-6.4	-6.8	-7.0	-6.7	**20-19**	15.6	13.7	14.1	14.9	*13.0*

	16-15	16.2	*13.5*	*13.9*	*14.2*	*13.5*	**17-16**	-10.1	-8.5	-9.4	-9.4	-9.5	**23-17**	-2.9	-3.1	-2.1	-2.1	-1.9
	15-11	-6.7	-6.1	-4.8	-5.0	*-4.4*	**21-15**	-7.2	-6.0	-6.5	-6.7	-6.4	**22-21**	-5.8	-5.0	-4.5	-4.6	-4.2
	11-10	-7.0	-5.9	-5.5	-5.5	-5.2	**13-11**	-3.9	-3.4	-4.2	-4.2	-4.1	**14-13**	13.8	*11.6*	12.0	12.2	11.8
	10-7	15.6	*13.2*	*13.3*	*13.5*	*13.0*	**12-10**	-6.8	-5.5	-6.5	-6.4	-6.6	**24-12**	-6.2	-5.9	-4.9	-4.9	-4.6
	7-3	16.1	*13.2*	*13.8*	*14.0*	*13.5*	**8-7**	-10.6	-9.2	-9.4	-9.7	-9.2	**9-8**	-3.5	-3.0	-2.6	-2.7	-2.4
	RMSD		2.0	*2.1*	1.8	*2.4*	*RMSD*		1.2	0.6	0.6	0.8	*RMSD*		1.3	1.3	1.0	2.0
2	**3-4**	-6.7	-5.9	-5.0	-5.0	-4.9	**2-3**	-7.5	-6.3	-7.4	-7.4	-7.3	**1-2**	13.8	12.3	12.7	12.7	12.6
	4-18	-7.5	-6.4	-5.8	-5.7	-5.6	**5-4**	-4.6	-3.9	-4.7	-4.8	-4.5	**6-5**	11.6	10.4	10.7	10.7	10.2
	18-16	15.7	*13.1*	*13.2*	*13.2*	*13.2*	**19-18**	-7.4	-6.4	-6.7	-6.8	-6.8	**20-19**	15.6	13.7	14.3	14.3	14.1
	16-15	16.2	*13.5*	*14.0*	*14.0*	*13.9*	**17-16**	-10.1	-8.5	-9.4	-9.4	-9.4	**23-17**	-2.9	-3.1	-2.1	-2.1	-2.0
	15-11	-6.7	-6.1	-4.9	-4.9	-4.7	**21-15**	-7.2	-6.0	-6.4	-6.5	-6.6	**22-21**	-5.8	-5.0	-4.6	-4.7	-4.4
	11-10	-7.0	-5.9	-5.6	-5.6	-5.4	**13-11**	-3.9	-3.4	-4.2	-4.2	-4.2	**14-13**	13.8	*11.6*	12.1	12.1	12.0
	10-7	15.6	*13.2*	*13.4*	*13.4*	*13.3*	**12-10**	-6.8	-5.5	-6.4	-6.4	-6.5	**24-12**	-6.2	-5.9	-5.0	-4.9	-4.8
	7-3	16.1	*13.2*	*13.9*	*13.9*	*13.8*	**8-7**	-10.6	-9.2	-9.4	-9.4	-9.5	**9-8**	-3.5	-3.0	-2.7	-2.7	-2.6
	RMSD		2.0	2.0	2.0	*2.1*	*RMSD*		1.2	0.7	0.6	0.6	*RMSD*		1.3	1.2	1.2	1.3

Table 5. Average torsional-angle values $<\varphi>$ and torsional-angle root- mean-square fluctuations *RMSF(φ)* obtained for cyclo-octane as calculated from 24 bond-vector RDC-restraining *rSD* simulations with γ^{SD} = 0.24 ps^{-1} for all 24 bond vectors $\vec{r}_{k_1k_2}$(***k₁-k₂***), see Figure 1. The molecular rotational-sampling (*MRS*) simulation[23] and the alignment-tensor (*AT*) simulations are t^{SD} = 20 μs long. The *MRS* restraining function parameter values are K^{RDC} = 2 kJmol^{-1}Hz^{-2}, τ_θ^{RDC} = 1 ns, and ΔD^0 = 1 Hz. The *AT* RDC-restraining function parameter values are K^{RDC} = **0.01 kJmol^{-1}Hz^{-2}**, τ_D^{RDC} = **0 ps**, and ΔD^0 = 1 Hz. τ_{AT}^{RDC} is varied. The atom numbers *(k1-k2-k3-k4)* defining a torsional angle are given in Figure 1. The $D_{k_1k_2}^0$ target values for the 24 bond vectors used in the RDC-restraining simulations were obtained from orientation-biasing *bSD* simulations[23] with γ^{SD} = 0.24 ps^{-1} and t^{SD} = 20 μs using the orientation-biasing function parameter values K^{bias} = 0.2 kJmol^{-1} and θ_{bias}^0 = 0°. In all simulations the GROMOS force field (***GR***) was used.

Torsional angle *(k1-k2-k3-k4)* backbone	Type of restraining *rSD* simulation							
	MRS		*AT*					
			τ_{AT}^{RDC} = 0 ps		τ_{AT}^{RDC} = 10 ps		τ_{AT}^{RDC} = 100 ps	
	<φ> (°)	*RMSF(φ)* (°)	*<φ>* (°)	*RMSF(φ)* (°)	*<φ>* (°)	*RMSF(φ)* (°)	*<φ>* (°)	*RMSF(φ)* (°)
7-3-4-5	-89	17	-97	26	-90	18	-89	17
4-3-7-10	-51	6	-51	6	-51	6	-51	6
5-4-18-16	90	17	98	25	91	18	90	17
3-7-10-11	48	6	49	7	48	7	48	7
7-10-11-15	-49	6	-48	7	-49	7	-49	7
10-11-15-16	49	7	48	7	49	7	49	7

11-15-16-18	-47	7	-48	7	-47	7	-47	7
15-16-18-4	50	6	50	7	50	6	50	6
side chain								
1-2-3-4	-83	28	-95	40	-84	30	-83	29
3-4-5-6	-71	44	-51	65	-69	47	-70	45
3-7-8-9	77	21	78	22	78	21	77	21
7-10-12-24	-78	22	-76	18	-77	22	-78	22
10-11-13-14	80	26	80	28	80	26	80	26
16-15-21-22	80	26	77	21	80	26	80	26
18-16-17-23	-77	22	-78	23	-78	22	-77	22
4-18-19-20	80	26	90	40	81	28	80	27

Table 6. Average torsional-angle values $<\varphi>$ and torsional-angle root-mean-square fluctuations *RMSF(φ)* obtained for cyclo-octane as calculated from 24 bond-vector RDC-restraining *rSD* simulations with γ^{SD} = 0.24 ps^{-1} for all 24 bond vectors $\vec{r}_{k_1k_2}$(**k_1-k_2**), see Figure 1. The molecular rotational-sampling (*MRS*) simulation[23] and the alignment-tensor (*AT*) simulations are t^{SD} = 20 μs long. The *MRS* restraining function parameter values are K^{RDC} = 2 kJmol^{-1}Hz^{-2}, τ_θ^{RDC} = 1 ns, and ΔD^0 = 1 Hz. The *AT* RDC-restraining function parameter values are K^{RDC} = **2 kJmol^{-1}Hz^{-2}**, τ_D^{RDC} = **100 ps**, and ΔD^0 = 1 Hz. τ_{AT}^{RDC} is varied. The atom numbers *(k1-k2-k3-k4)* defining a torsional angle are given in Figure 1. The $D^0_{k_1k_2}$ target values for the 24 bond vectors used in the RDC-restraining simulations were obtained from orientation-biasing *bSD* simulations[23] with γ^{SD} = 0.24 ps^{-1} and t^{SD} = 20 μs using the orientation-biasing function parameter values K^{bias} = 0.2 kJmol^{-1} and θ^0_{bias} = 0°. In all simulations the GROMOS force field (***GR***) was used.

Torsional angle *(k1-k2-k3-k4)* backbone	Type of restraining *rSD* simulation							
	MRS		*AT*					
			τ_{AT}^{RDC} = 0 ps		τ_{AT}^{RDC} = 10 ps		τ_{AT}^{RDC} = 100 ps	
	<φ> (°)	*RMSF(φ)* (°)	*<φ>* (°)	*RMSF(φ)* (°)	*<φ>* (°)	*RMSF(φ)* (°)	*<φ>* (°)	*RMSF(φ)* (°)
7-3-4-5	-89	17	-89	17	-89	17	-89	18
4-3-7-10	-51	6	-51	6	-51	6	-51	6
5-4-18-16	90	17	90	17	90	17	90	17
3-7-10-11	48	6	48	7	48	7	48	7
7-10-11-15	-49	6	-49	7	-49	7	-49	7
10-11-15-16	49	7	49	7	49	7	49	7

11-15-16-18	-47	7	-47	7	-47	7	-47	7
15-16-18-4	50	6	50	6	50	6	50	6
side chain								
1-2-3-4	-83	28	-83	29	-83	29	-84	29
3-4-5-6	-71	44	-70	45	-71	45	-70	45
3-7-8-9	77	21	77	21	77	21	77	22
7-10-12-24	-78	22	-78	22	-78	22	-78	22
10-11-13-14	80	26	80	26	80	26	80	26
16-15-21-22	80	26	80	27	80	27	80	27
18-16-17-23	-77	22	-77	22	-78	22	-77	22
4-18-19-20	80	26	80	27	80	26	80	27

Table 7. Root-mean-square deviations (*RMSD*) of the RDC-values $< D_{k_1k_2} >_{t^{SD}}$ from their target values $D^0_{k_1k_2}$ averaged over the eight RDCs of the bonds in the ring, the first side-chain bonds and the second side-chain bonds in cyclo-octane. The $< D_{k_1k_2} >_{t^{SD}}$ values (Hz) were calculated from 24 bond-vector RDC-restraining t^{SD} = 30 ns *AT rSD* simulations with γ^{SD} = 0.24 ps^{-1} for all 24 bond vectors $\vec{r}_{k_1k_2}$ (***k₁-k₂***), see Figure 1. The *AT* RDC-restraining function parameter values K^{RDC}, τ_D^{RDC} and τ_{AT}^{RDC} are varied, ΔD^0 = 1 Hz. The $D^0_{k_1k_2}$ target values for the 24 bond vectors were obtained from orientation-biasing *bSD* simulations[23] with γ^{SD} = 0.24 ps^{-1} and t^{SD} = 20 μs using the orientation-biasing function parameter values K^{bias} = 0.2 kJmol^{-1} and θ^0_{bias} = 0°. In all simulations the GROMOS force field without torsional-angle terms (***GRnt***) was used. *RMSD* values larger than 2 Hz are in italics. "-": Result not available due to SHAKE failure: too large forces.

τ_D^{RDC} (ps)	K^{RDC} (kJmol^{-1} Hz^{-2})	*RMSD* ($< D_{k_1k_2} >_{t^{SD}}$ - $D^0_{k_1k_2}$) (Hz)														
		Backbone bonds					First side-chain bonds					Second side-chain bonds				
		AT: τ_{AT}^{RDC} (ps)					*AT:* τ_{AT}^{RDC} (ps)					*AT:* τ_{AT}^{RDC} (ps)				
		0	1	10	10^2	10^3	0	1	10	10^2	10^3	0	1	10	10^2	10^3
0	0.01	*2.3*	*2.3*	*2.3*	*2.3*	*2.3*	1.3	1.3	1.4	1.4	1.4	2.0	1.5	1.4	1.3	1.6
	0.02	*2.4*	*2.3*	*2.3*	*2.3*	*2.3*	1.5	1.2	1.4	1.4	1.4	*2.9*	1.7	1.4	1.4	1.4
	0.05	*3.2*	*2.4*	*2.4*	*2.3*	*2.3*	*2.7*	1.3	1.4	1.3	1.4	*5.6*	2.0	1.5	1.4	1.3
	0.1	*4.7*	*2.6*	*2.4*	*2.3*	*2.3*	*4.5*	1.4	1.4	1.4	1.4	*9.1*	*2.5*	1.6	1.5	1.5
	0.2	*5.1*	*2.9*	*2.6*	*2.4*	*2.3*	*4.6*	1.9	1.8	1.4	1.4	*9.5*	*3.8*	*2.6*	1.5	1.4
	0.5	-	*3.8*	*3.3*	*2.4*	*2.4*	-	*4.0*	*3.3*	1.6	1.4	-	*6.2*	*5.1*	1.6	1.5
1	0.2	*2.3*	*2.3*	*2.3*	*2.3*	*2.3*	1.4	1.4	1.4	1.4	1.4	1.3	1.4	1.3	1.6	1.4

	0.5	*2.3*	*2.3*	*2.3*	*2.3*	*2.3*	1.4	1.4	1.4	1.4	1.4	1.5	1.6	1.6	1.4	1.4
	1.0	*2.3*	*2.3*	*2.3*	*2.3*	*2.3*	1.4	1.4	1.4	1.4	1.4	1.4	1.5	1.4	1.4	1.5
10	0.2	*2.3*	*2.3*	*2.3*	*2.3*	*2.3*	1.4	1.4	1.4	1.4	1.4	1.4	1.4	1.3	1.3	1.4
	0.5	*2.3*	*2.3*	*2.3*	*2.3*	*2.3*	1.4	1.4	1.4	1.4	1.4	1.3	1.4	1.4	1.3	1.4
	1	*2.3*	*2.3*	*2.3*	*2.3*	*2.3*	1.4	1.4	1.4	1.4	1.4	1.4	1.4	1.3	1.4	1.5
100	0.2	*2.3*	*2.4*	*2.3*	*2.3*	*2.3*	1.4	1.4	1.4	1.4	1.4	1.4	1.5	1.6	1.4	1.5
	0.5	*2.3*	*2.3*	*2.3*	*2.3*	*2.3*	1.4	1.4	1.4	1.4	1.4	1.5	1.4	1.5	1.4	1.4
	1	*2.3*	*2.3*	*2.3*	*2.3*	*2.3*	1.4	1.4	1.4	1.4	1.4	1.4	1.3	1.5	1.4	1.4
	2	*2.3*	*2.3*	*2.3*	*2.3*	*2.3*	1.4	1.4	1.4	1.4	1.3	1.4	1.4	1.4	1.6	1.5
	5	*2.3*	*2.3*	*2.3*	*2.3*	*2.3*	1.4	1.4	1.4	1.4	1.4	1.4	1.3	1.4	1.5	1.4
1000	1	*2.3*	*2.3*	*2.3*	*2.3*	*2.3*	1.4	1.4	1.4	1.4	1.4	1.5	1.4	1.4	1.4	1.4
	2	*2.3*	*2.3*	*2.3*	*2.3*	*2.3*	1.3	1.4	1.4	1.4	1.4	1.5	1.5	1.4	1.4	1.5
	5	*2.3*	*2.3*	*2.3*	*2.3*	*2.3*	1.4	1.4	1.3	1.4	1.4	1.4	1.5	1.5	1.3	1.4
	10	*2.3*	*2.3*	*2.3*	*2.3*	*2.3*	1.3	1.4	1.3	1.4	1.4	1.4	1.3	1.4	1.4	1.4
	100	*2.3*	*2.3*	*2.3*	*2.3*	*2.3*	1.4	1.4	1.4	1.4	1.4	1.3	1.4	1.7	1.4	1.5

Table 8. Average GROMOS force-field potential energy E_{pot} and RDC-restraining energy E_{AT}^{RDC} in cyclo-octane calculated from 24 bond-vector RDC-restraining *AT rSD* simulations of length t^{SD} = 30 ns with γ^{SD} = 0.24 ps^{-1} for all 24 bond vectors $\vec{r}_{k_1k_2}$ (***k*₁-*k*₂**), see Figure 1. The *AT* RDC-restraining function parameter values K^{RDC}, τ_D^{RDC} and τ_{AT}^{RDC} are varied, ΔD^0 = 1 Hz. The $D^0_{k_1k_2}$ target values for the 24 bond vectors were obtained from orientation-biasing *bSD* simulations[23] with γ^{SD} = 0.24 ps^{-1} and t^{SD} = 20 μs using the orientation-biasing function parameter values K^{bias} = 0.2 kJmol^{-1} and θ^0_{bias} = 0°. In all simulations the GROMOS force field without torsional-angle terms (***GRnt***) was used. "-": Result not available due to SHAKE failure: too large forces.

τ_D^{RDC} (ps)	K^{RDC} (kJmol^{-1} Hz^{-2})	Potential energy (kJ/mol)									
		GROMOS molecular energy E_{pot}					RDC-restraining energy E_{AT}^{RDC}				
		AT: τ_{AT}^{RDC} (ps)					*AT:* τ_{AT}^{RDC} (ps)				
		0	1	10	10^2	10^3	0	1	10	10^2	10^3
0	0.01	35	35	35	36	35	1	1	1	1	1
	0.02	36	36	35	36	35	3	3	3	3	3
	0.05	42	38	36	35	35	14	8	7	7	7
	0.1	53	42	37	36	36	47	17	14	13	14
	0.2	81	57	44	36	36	101	45	37	27	28
	0.5	-	126	68	38	41	-	184	152	72	70
1	0.2	35	35	35	35	36	12	12	12	12	12
	0.5	36	35	36	35	35	31	32	32	30	30
	1.0	35	35	35	36	35	60	62	60	61	62
10	0.2	35	35	35	35	36	10	9	10	10	10
	0.5	35	35	35	35	35	24	24	24	23	24

	1	35	35	35	35	35	48	49	47	50	50
100	0.2	35	36	36	35	36	4	5	5	5	5
	0.5	35	35	35	35	35	13	13	12	12	13
	1	35	35	35	35	35	26	24	24	24	26
	2	35	35	35	35	35	48	50	48	50	46
	5	35	35	35	35	35	119	124	124	129	120
1000	1	35	35	36	35	35	12	12	12	13	12
	2	35	35	36	35	36	26	26	24	25	25
	5	35	36	35	35	35	59	68	64	60	62
	10	35	35	35	35	35	124	124	120	131	127
	100	35	35	35	35	36	1227	1179	1474	1224	1254

Table 9. RDC $< D_{k_1k_2} >_{t^{SD}}$ values (Hz) obtained for cyclo-octane as calculated from 24 bond-vector RDC-restraining *rSD* simulations with γ^{SD} = 0.24 ps^{-1} for all 24 bond vectors $\vec{r}_{k_1k_2}$(***k*₁-*k*₂**), see Figure 1. *RMSD*: root-mean-square difference between $< D_{k_1k_2} >_{t^{SD}}$ and $D^0_{k_1k_2}$ for the eight bond-vector RDCs. The molecular rotational-sampling (*MRS*) simulation[23] is t^{SD} = 20 μs long, while the alignment-tensor (*AT*) simulations are t^{SD} = 30 ns long. The *MRS* RDC-restraining function parameter values are K^{RDC} = 2 kJmol^{-1}Hz^{-2}, τ_θ^{RDC} = 1 ns, and ΔD^0 = 1 Hz. The *AT* RDC-restraining function parameter values K^{RDC} and τ_{AT}^{RDC} are varied and τ_D^{RDC} = **0 ps**, ΔD^0 = 1 Hz. The sequence numbers of the atoms are given in Figure 1. The $D^0_{k_1k_2}$ target values for the 24 bond vectors were obtained from orientation-biasing *bSD* simulations[23] with γ^{SD} = 0.24 ps^{-1} and t^{SD} = 20 μs using the orientation-biasing function parameter values K^{bias} = 0.2 kJmol^{-1} and θ^0_{bias} = 0°. In all simulations the GROMOS force field without torsional-angle terms (***GRnt***) was used. Deviations of averaged RDC-values $< D_{k_1k_2} >_{t^{SD}}$ from their target values $D^0_{k_1k_2}$ larger than 2 Hz are in italics.

AT: K^{RDC} (kJmol^{-1} Hz^{-2})	Backbone bonds						First side-chain bonds						Second side-chain bonds					
	Bond vector $\vec{r}_{k_1k_2}$	$D^0_{k_1k_2}$ (Hz)	$< D_{k_1k_2} >_{t^{SD}}$ (Hz)				Bond vector $\vec{r}_{k_1k_2}$	$D^0_{k_1k_2}$ (Hz)	$< D_{k_1k_2} >_{t^{SD}}$ (Hz)				Bond vector $\vec{r}_{k_1k_2}$	$D^0_{k_1k_2}$ (Hz)	$< D_{k_1k_2} >_{t^{SD}}$ (Hz)			
			MRS	*AT:* τ_{AT}^{RDC} (ps)					*MRS*	*AT:* τ_{AT}^{RDC} (ps)					*MRS*	*AT:* τ_{AT}^{RDC} (ps)		
			-	0	10	100			-	0	10	100			-	0	10	100
0.01	**3-4**	-5.4	-5.0	-4.1	-4.1	-4.1	**2-3**	-8.3	-6.8	-7.1	-7.3	-7.2	**1-2**	2.0	1.9	1.3	2.0	2.0
	4-18	-6.3	-5.6	-4.9	-4.9	-4.9	**5-4**	6.2	5.4	7.0	5.6	5.6	**6-5**	4.7	4.4	*1.0*	4.1	4.0
	18-16	15.1	*12.4*	*12.0*	*11.8*	*11.9*	**19-18**	-8.2	-6.9	-7.0	-7.2	-7.1	**20-19**	3.4	2.7	2.2	2.9	2.9

	16-15	16.5	*13.5*	*13.5*	*13.6*	*13.6*	**17-16**	-10.7	-8.8	-8.9	-8.8	-8.8	**23-17**	-7.5	-6.8	-5.9	-5.9	-5.9
	15-11	-5.1	-4.9	-3.9	-4.0	-4.0	**21-15**	-7.1	-5.9	-5.8	-5.4	-5.4	**22-21**	4.1	3.7	2.9	3.4	3.5
	11-10	-5.8	-5.1	-4.6	-4.7	-4.7	**13-11**	-4.6	-3.9	-4.0	-4.6	-4.6	**14-13**	17.6	*15.2*	*14.4*	*14.6*	*14.8*
	10-7	15.6	*13.0*	*12.7*	*12.8*	*12.8*	**12-10**	-6.8	-5.5	-5.4	-5.1	-5.0	**24-12**	5.1	4.3	3.8	4.3	4.3
	7-3	15.9	*12.8*	*12.7*	*12.6*	*12.6*	**8-7**	-10.9	-9.3	-9.1	-9.1	-9.0	**9-8**	-7.2	-6.1	-5.9	-5.9	-5.9
	RMSD		*2.1*	*2.3*	*2.3*	*2.3*	*RMSD*		1.3	1.3	1.4	1.4	*RMSD*		1.1	2.0	1.4	1.3
0.05	**3-4**	-5.4	-5.0	-3.8	-4.1	-4.1	**2-3**	-8.3	-6.8	-6.8	-7.3	-7.2	**1-2**	2.0	1.9	*-0.8*	1.8	1.9
	4-18	-6.3	-5.6	-4.5	-4.8	-4.9	**5-4**	6.2	5.4	*9.6*	5.7	6.0	**6-5**	4.7	4.4	*-3.2*	4.0	3.2
	18-16	15.1	*12.4*	*10.6*	*11.8*	*11.9*	**19-18**	-8.2	-6.9	-6.6	-7.2	-7.1	**20-19**	3.4	2.7	*-0.2*	2.7	2.8
	16-15	16.5	*13.5*	*12.5*	*13.6*	*13.5*	**17-16**	-10.7	-8.8	*-8.0*	-8.9	-8.8	**23-17**	-7.5	-6.8	-5.7	-5.9	-5.9
	15-11	-5.1	-4.9	-3.5	-4.0	-4.0	**21-15**	-7.1	-5.9	*-5.0*	-5.4	-5.5	**22-21**	4.1	3.7	*-0.1*	3.2	3.4
	11-10	-5.8	-5.1	-4.2	-4.7	-4.7	**13-11**	-4.6	-3.9	*-0.6*	-4.5	-4.4	**14-13**	17.6	*15.2*	*6.6*	*14.5*	*14.7*
	10-7	15.6	*13.0*	*11.8*	*12.8*	*12.7*	**12-10**	-6.8	-5.5	*-4.6*	-5.1	-5.1	**24-12**	5.1	4.3	*0.5*	4.1	4.4
	7-3	15.9	*12.8*	*11.2*	*12.6*	*12.6*	**8-7**	-10.9	-9.3	*-8.0*	-9.1	-9.0	**9-8**	-7.2	-6.1	-5.7	-5.9	-5.9
	RMSD		*2.1*	*3.2*	*2.4*	*2.3*	*RMSD*		1.3	*2.7*	1.4	1.3	*RMSD*		1.1	*5.6*	1.5	1.4
0.1	**3-4**	-5.4	-5.0	*-3.3*	-4.0	-4.1	**2-3**	-8.3	-6.8	*-6.2*	-7.4	-7.1	**1-2**	2.0	1.9	*-2.2*	1.7	1.9
	4-18	-6.3	-5.6	*-4.1*	-4.8	-4.9	**5-4**	6.2	5.4	*10.1*	5.6	6.0	**6-5**	4.7	4.4	*-3.1*	4.4	3.0
	18-16	15.1	*12.4*	*7.9*	*11.7*	*11.9*	**19-18**	-8.2	-6.9	*-6.0*	-7.3	-7.1	**20-19**	3.4	2.7	*-1.7*	2.6	2.8
	16-15	16.5	*13.5*	*11.0*	*13.6*	*13.5*	**17-16**	-10.7	-8.8	*-6.2*	-8.9	-8.8	**23-17**	-7.5	-6.8	*-5.3*	-5.9	-6.0
	15-11	-5.1	-4.9	-3.2	-3.9	-4.0	**21-15**	-7.1	-5.9	*-3.0*	-5.3	-5.5	**22-21**	4.1	3.7	*-2.6*	2.9	3.3
	11-10	-5.8	-5.1	-4.1	-4.6	-4.7	**13-11**	-4.6	-3.9	*3.3*	-4.4	-4.4	**14-13**	17.6	*15.2*	*-3.6*	*14.0*	*14.7*
	10-7	15.6	*13.0*	*10.3*	*12.8*	*12.7*	**12-10**	-6.8	-5.5	*-2.7*	-5.0	-5.2	**24-12**	5.1	4.3	*-2.1*	3.8	4.3
	7-3	15.9	*12.8*	*8.7*	*12.5*	*12.7*	**8-7**	-10.9	-9.3	*-6.2*	-9.0	-9.1	**9-8**	-7.2	-6.1	*-5.3*	-5.8	-5.9
	RMSD		*2.1*	*4.7*	*2.4*	*2.3*	*RMSD*		1.3	*4.5*	1.4	1.4	*RMSD*		1.1	*9.1*	1.6	1.5
0.2	**3-4**	-5.4	-5.0	-3.2	-4.0	-4.1	**2-3**	-8.3	-6.8	*-5.7*	-7.2	-7.2	**1-2**	2.0	1.9	*-2.6*	1.4	1.9
	4-18	-6.3	-5.6	-3.9	-4.8	-4.9	**5-4**	6.2	5.4	*9.4*	5.7	5.8	**6-5**	4.7	4.4	*-3.7*	4.6	3.5

	18-16	15.1	*12.4*	*7.6*	*11.3*	*11.8*	**19-18**	-8.2	-6.9	*-5.5*	-7.1	-7.1	**20-19**	3.4	2.7	*-2.5*	2.2	2.9
	16-15	16.5	*13.5*	*10.3*	*13.4*	*13.5*	**17-16**	-10.7	-8.8	*-6.0*	*-8.5*	-8.8	**23-17**	-7.5	-6.8	*-4.9*	-5.8	-5.9
	15-11	-5.1	-4.9	-3.1	-3.9	-4.0	**21-15**	-7.1	-5.9	*-3.0*	*-4.8*	-5.5	**22-21**	4.1	3.7	*-3.1*	2.0	3.4
	11-10	-5.8	-5.1	-3.9	-4.6	-4.7	**13-11**	-4.6	-3.9	*3.3*	-3.7	-4.4	**14-13**	17.6	*15.2*	*-4.2*	*11.5*	*14.5*
	10-7	15.6	*13.0*	*9.6*	*12.6*	*12.7*	**12-10**	-6.8	-5.5	*-2.6*	*-4.4*	-5.1	**24-12**	5.1	4.3	*-2.9*	*2.8*	4.2
	7-3	15.9	*12.8*	*8.3*	*12.0*	*12.6*	**8-7**	-10.9	-9.3	*-6.0*	*-8.7*	-9.0	**9-8**	-7.2	-6.1	*-4.8*	-5.8	-5.9
	RMSD		*2.1*	*5.1*	*2.6*	*2.4*	*RMSD*		1.3	*4.6*	1.8	1.4	*RMSD*		1.1	*9.5*	*2.6*	1.5

Table 10. RDC $< D_{k_1k_2} >_{t^{SD}}$ values (Hz) obtained for cyclo-octane as calculated from 24 bond-vector RDC-restraining *rSD* simulations with γ^{SD} = 0.24 ps^{-1} for all 24 bond vectors $\vec{r}_{k_1k_2}$(**k_1-k_2**), see Figure 1. *RMSD*: root-mean-square difference between $< D_{k_1k_2} >_{t^{SD}}$ and $D^0_{k_1k_2}$ for the eight bond-vector RDCs. The molecular rotational-sampling (*MRS*) simulation[23] is t^{SD} = 20 μs long, while the alignment-tensor (*AT*) simulations are t^{SD} = 30 ns long. The *MRS* RDC-restraining function parameter values are K^{RDC} = 2 kJmol^{-1}Hz^{-2}, τ_θ^{RDC} = 1 ns, and ΔD^0 = 1 Hz. The *AT* RDC-restraining function parameter values K^{RDC} and τ_{AT}^{RDC} are varied and τ_D^{RDC} = **100 ps**, ΔD^0 = 1 Hz. The sequence numbers of the atoms are given in Figure 1. The $D^0_{k_1k_2}$ target values for the 24 bond vectors were obtained from orientation-biasing *bSD* simulations[23] with γ^{SD} = 0.24 ps^{-1} and t^{SD} = 20 μs using the orientation-biasing function parameter values K^{bias} = 0.2 kJmol^{-1} and θ^0_{bias} = 0°. In all simulations the GROMOS force field without torsional-angle terms (***GRnt***) was used. Deviations of averaged RDC-values $< D_{k_1k_2} >_{t^{SD}}$ from their target values $D^0_{k_1k_2}$ larger than 2 Hz are in italics.

AT: K^{RDC} (kJmol^{-1} Hz^{-2})	Backbone bonds						First side-chain bonds						Second side-chain bonds					
	Bond vector $\vec{r}_{k_1k_2}$	$D^0_{k_1k_2}$ (Hz)	$< D_{k_1k_2} >_{t^{SD}}$ (Hz)				Bond vector $\vec{r}_{k_1k_2}$	$D^0_{k_1k_2}$ (Hz)	$< D_{k_1k_2} >_{t^{SD}}$ (Hz)				Bond vector $\vec{r}_{k_1k_2}$	$D^0_{k_1k_2}$ (Hz)	$< D_{k_1k_2} >_{t^{SD}}$ (Hz)			
			MRS	*AT:* τ_{AT}^{RDC} (ps)					*MRS*	*AT:* τ_{AT}^{RDC} (ps)					*MRS*	*AT:* τ_{AT}^{RDC} (ps)		
			-	0	10	100			-	0	10	100			-	0	10	100
1	**3-4**	-5.4	-5.0	-4.1	-4.2	-4.1	**2-3**	-8.3	-6.8	-7.2	-7.1	-7.1	**1-2**	2.0	1.9	2.0	1.9	1.9
	4-18	-6.3	-5.6	-4.9	-5.0	-4.9	**5-4**	6.2	5.4	5.9	6.1	6.0	**6-5**	4.7	4.4	3.4	2.9	3.0
	18-16	15.1	*12.4*	*11.9*	*11.9*	*11.9*	**19-18**	-8.2	-6.9	-7.1	-7.1	-7.0	**20-19**	3.4	2.7	2.9	2.9	2.9

	16-15	16.5	*13.5*	*13.5*	*13.5*	*13.5*	**17-16**	-10.7	-8.8	-8.8	-8.8	-8.8	**23-17**	-7.5	-6.8	-6.0	-6.0	-6.0
	15-11	-5.1	-4.9	-4.0	-4.0	-4.0	**21-15**	-7.1	-5.9	-5.5	-5.5	-5.5	**22-21**	4.1	3.7	3.5	3.4	3.4
	11-10	-5.8	-5.1	-4.7	-4.7	-4.7	**13-11**	-4.6	-3.9	-4.5	-4.3	-4.4	**14-13**	17.6	*15.2*	*14.7*	*14.7*	*14.7*
	10-7	15.6	*13.0*	*12.7*	*12.7*	*12.7*	**12-10**	-6.8	-5.5	-5.1	-5.1	-5.2	**24-12**	5.1	4.3	4.4	4.3	4.3
	7-3	15.9	*12.8*	*12.6*	*12.6*	*12.6*	**8-7**	-10.9	-9.3	-9.0	-9.0	-9.0	**9-8**	-7.2	-6.1	-5.9	-5.9	-5.9
	RMSD		*2.1*	*2.3*	*2.3*	*2.3*	*RMSD*		1.3	1.4	1.4	1.4	*RMSD*		1.1	1.4	1.5	1.4
2	**3-4**	-5.4	-5.0	-4.1	-4.1	-4.2	**2-3**	-8.3	-6.8	-7.2	-7.2	-7.1	**1-2**	2.0	1.9	2.0	2.0	1.9
	4-18	-6.3	-5.6	-4.9	-4.9	-4.9	**5-4**	6.2	5.4	5.8	5.8	6.3	**6-5**	4.7	4.4	3.6	3.6	*2.4*
	18-16	15.1	*12.4*	*11.9*	*11.9*	*11.9*	**19-18**	-8.2	-6.9	-7.1	-7.1	-7.0	**20-19**	3.4	2.7	2.9	2.9	2.8
	16-15	16.5	*13.5*	*13.5*	*13.6*	*13.5*	**17-16**	-10.7	-8.8	-8.8	-8.8	-8.8	**23-17**	-7.5	-6.8	-5.9	-5.9	-5.9
	15-11	-5.1	-4.9	-4.0	-4.0	-4.0	**21-15**	-7.1	-5.9	-5.5	-5.5	-5.6	**22-21**	4.1	3.7	3.5	3.4	3.5
	11-10	-5.8	-5.1	-4.7	-4.7	-4.7	**13-11**	-4.6	-3.9	-4.5	-4.5	-4.3	**14-13**	17.6	*15.2*	*14.7*	*14.7*	*14.7*
	10-7	15.6	*13.0*	*12.8*	*12.7*	*12.7*	**12-10**	-6.8	-5.5	-5.1	-5.1	-5.2	**24-12**	5.1	4.3	4.3	4.4	4.3
	7-3	15.9	*12.8*	*12.6*	*12.6*	*12.6*	**8-7**	-10.9	-9.3	-9.0	-9.0	-9.0	**9-8**	-7.2	-6.1	-5.9	-5.9	-5.9
	RMSD		*2.1*	*2.3*	*2.3*	*2.3*	*RMSD*		1.3	1.4	1.4	1.4	*RMSD*		1.1	1.4	1.4	1.6

Table 11. Average torsional-angle values $<\varphi>$ and torsional-angle root- mean-square fluctuations *RMSF(φ)* obtained for cyclo-octane as calculated from 24 bond-vector RDC-restraining *rSD* simulations with γ^{SD} = 0.24 ps^{-1} for all 24 bond vectors $\vec{r}_{k_1k_2}$(**k_1-k_2**), see Figure 1. The molecular rotational-sampling (*MRS*) simulation[23] and the alignment-tensor (*AT*) simulations are t^{SD} = 20 μs long. The *MRS* restraining function parameter values are K^{RDC} = 2 kJmol^{-1}Hz^{-2}, τ_θ^{RDC} = 1 ns, and ΔD^0 = 1 Hz. The *AT* RDC-restraining function parameter values are K^{RDC} = **0.01 kJmol^{-1}Hz^{-2}**, τ_D^{RDC} = **0 ps**, and ΔD^0 = 1 Hz. τ_{AT}^{RDC} is varied. The atom numbers *(k1-k2-k3-k4)* defining a torsional angle are given in Figure 1. The $D_{k_1k_2}^0$ target values for the 24 bond vectors used in the RDC-restraining simulations were obtained from orientation-biasing *bSD* simulations[23] with γ^{SD} = 0.24 ps^{-1} and t^{SD} = 20 μs using the orientation-biasing function parameter values K^{bias} = 0.2 kJmol^{-1} and θ_{bias}^0 = 0°. In all simulations the GROMOS force field without torsional-angle terms (***GRnt***) was used.

Torsional angle *(k1-k2-k3-k4)* backbone	Type of restraining *rSD* simulation							
	MRS		*AT*					
			τ_{AT}^{RDC} = 0 ps		τ_{AT}^{RDC} = 10 ps		τ_{AT}^{RDC} = 100 ps	
	$<\varphi>$ (°)	*RMSF(φ)* (°)	$<\varphi>$ (°)	*RMSF(φ)* (°)	$<\varphi>$ (°)	*RMSF(φ)* (°)	$<\varphi>$ (°)	*RMSF(φ)* (°)
7-3-4-5	-116	18	-119	18	-117	18	-116	18
4-3-7-10	-43	11	-43	11	-43	11	-43	11
5-4-18-16	116	18	119	18	117	18	116	18
3-7-10-11	40	10	41	10	41	10	40	10
7-10-11-15	-40	11	-39	11	-40	11	-40	11
10-11-15-16	40	11	39	11	40	11	40	11

11-15-16-18	-40	10	-41	10	-41	10	-40	10
15-16-18-4	43	11	43	11	43	11	43	11
side chain								
1-2-3-4	-113	23	-115	24	-113	24	-113	24
3-4-5-6	-12	97	4	97	-11	97	-13	97
3-7-8-9	106	24	106	24	106	25	106	25
7-10-12-24	-104	25	-102	26	-104	25	-104	25
10-11-13-14	105	26	102	33	104	27	105	26
16-15-21-22	104	25	102	26	103	25	104	25
18-16-17-23	-106	24	-106	24	-106	24	-106	25
4-18-19-20	112	23	115	24	113	24	113	24

Table 12. Average torsional-angle values $<\varphi>$ and torsional-angle root- mean-square fluctuations *RMSF(φ)* obtained for cyclo-octane as calculated from 24 bond-vector RDC-restraining *rSD* simulations with γ^{SD} = 0.24 ps^{-1} for all 24 bond vectors $\vec{r}_{k_1k_2}$ ***k₁-k₂***), see Figure 1. The molecular rotational-sampling (*MRS*) simulation[23] and the alignment-tensor (*AT*) simulations are t^{SD} = 20 μs long. The *MRS* restraining function parameter values are K^{RDC} = 2 kJmol^{-1}Hz^{-2}, τ_θ^{RDC} = 1 ns, and ΔD^0 = 1 Hz. The *AT* RDC-restraining function parameter values are K^{RDC} = **2 kJmol^{-1}Hz^{-2}**, τ_D^{RDC} = **100 ps**, and ΔD^0 = 1 Hz. τ_{AT}^{RDC} is varied. The atom numbers *(k1-k2-k3-k4)* defining a torsional angle are given in Figure 1. The $D_{k_1k_2}^0$ target values for the 24 bond vectors used in the RDC-restraining simulations were obtained from orientation-biasing *bSD* simulations[23] with γ^{SD} = 0.24 ps^{-1} and t^{SD} = 20 μs using the orientation-biasing function parameter values K^{bias} = 0.2 kJmol^{-1} and θ_{bias}^0 = 0°. In all simulations the GROMOS force field without torsional-angle terms (***GRnt***) was used.

Torsional angle *(k1-k2-k3-k4)* backbone	Type of restraining *rSD* simulation							
	MRS		*AT*					
			τ_{AT}^{RDC} = 0 ps		τ_{AT}^{RDC} = 10 ps		τ_{AT}^{RDC} = 100 ps	
	$<\varphi>$ (°)	*RMSF(φ)* (°)	$<\varphi>$ (°)	*RMSF(φ)* (°)	$<\varphi>$ (°)	*RMSF(φ)* (°)	$<\varphi>$ (°)	*RMSF(φ)* (°)
7-3-4-5	-116	18	-116	18	-116	18	-116	18
4-3-7-10	-43	11	-43	11	-43	11	-43	11
5-4-18-16	116	18	116	18	116	18	116	18
3-7-10-11	40	10	40	10	40	10	40	10
7-10-11-15	-40	11	-40	11	-40	11	-40	11
10-11-15-16	40	11	40	11	40	11	40	11

11-15-16-18	-40	10	-40	10	-40	10	-40	10
15-16-18-4	43	11	43	11	43	11	43	11
side chain								
1-2-3-4	-113	23	-112	24	-112	24	-112	24
3-4-5-6	-12	97	-12	97	-13	97	-12	97
3-7-8-9	106	24	106	25	106	24	106	24
7-10-12-24	-104	25	-104	25	-104	25	-104	25
10-11-13-14	105	26	105	26	105	26	105	26
16-15-21-22	104	25	104	25	104	25	104	25
18-16-17-23	-106	24	-106	25	-106	25	-106	25
4-18-19-20	112	23	113	24	112	24	112	24

Figures

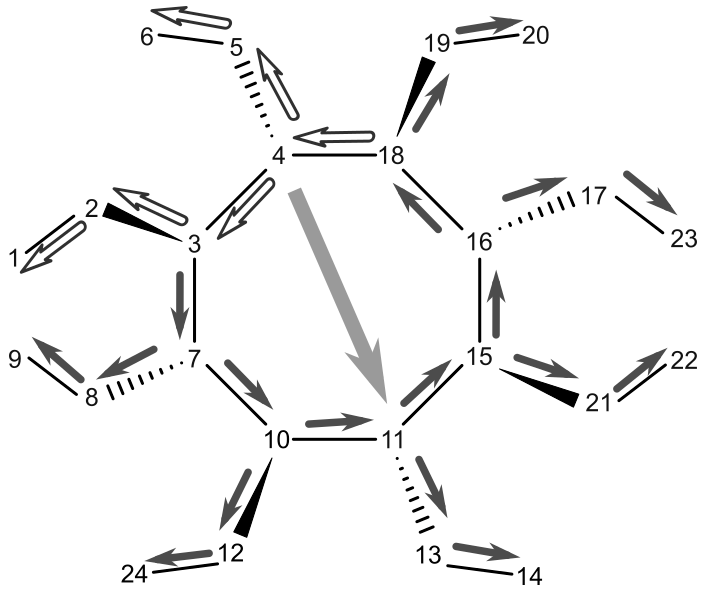


Figure 1. Molecular topology of the cyclo-octane molecule with eight side chains and with atom sequence numbers of the CH_1, CH_2, and CH_3 united atoms. The 24 small grey, open and solid, arrows indicate the 24 bond vectors, for which RDC values are calculated. The open arrows are bond vectors of which the motion is more extensively analysed. The large grey arrow indicates the atom-atom vector that was used in the biasing force used to generate an anisotropic orientation distribution of the molecule[23].

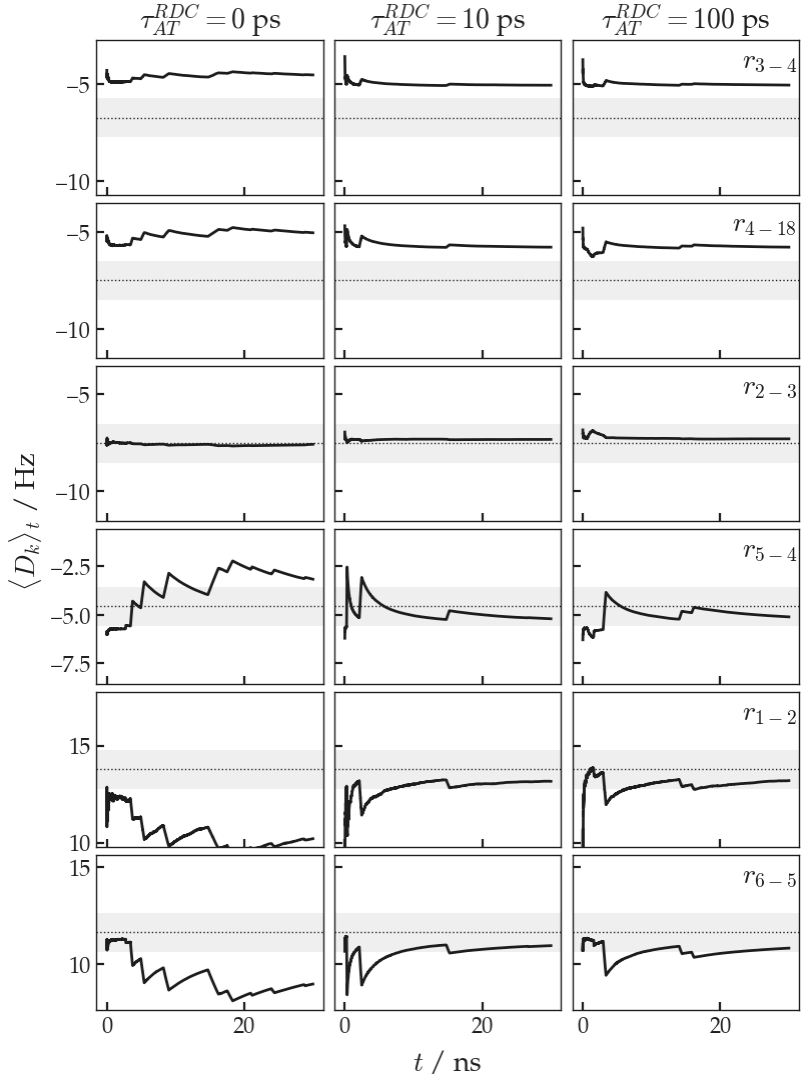


Figure 2. RDC $< D_{k_1 k_2} >_t$ values (Hz) as function of time *t* obtained for cyclo-octane as calculated from 24 bond-vector RDC-restraining *AT rSD* simulations with γ^{SD} = 0.24 ps^{-1} for all 24 bond vectors $\vec{r}_{k_1 k_2}$ (*k*1-*k*2), see Figure 1. The *AT* RDC-restraining function parameter values are K^{RDC} = **0.01 kJmol^{-1}Hz^{-2}** and τ_D^{RDC} = **0 ps** (solid lines), τ_{AT}^{RDC} = 0, 10, 100 ps (columns), and ΔD^0 = 1 Hz. The $D^0_{k_1 k_2}$ target values (dotted lines) were generated in *bSD* simulations[23] with K^{bias} = 0.2 kJmol^{-1} and θ^0_{bias} = 0°. The area $D^0_k \pm \Delta D^0$ is shaded. Six RDCs (rows) are shown (backbone 3-4 and 4-18; first side chain: 2-3 and 5-

4; second side chain: 1-2, 6-5). In all simulations the GROMOS force field (***GR***) was used.

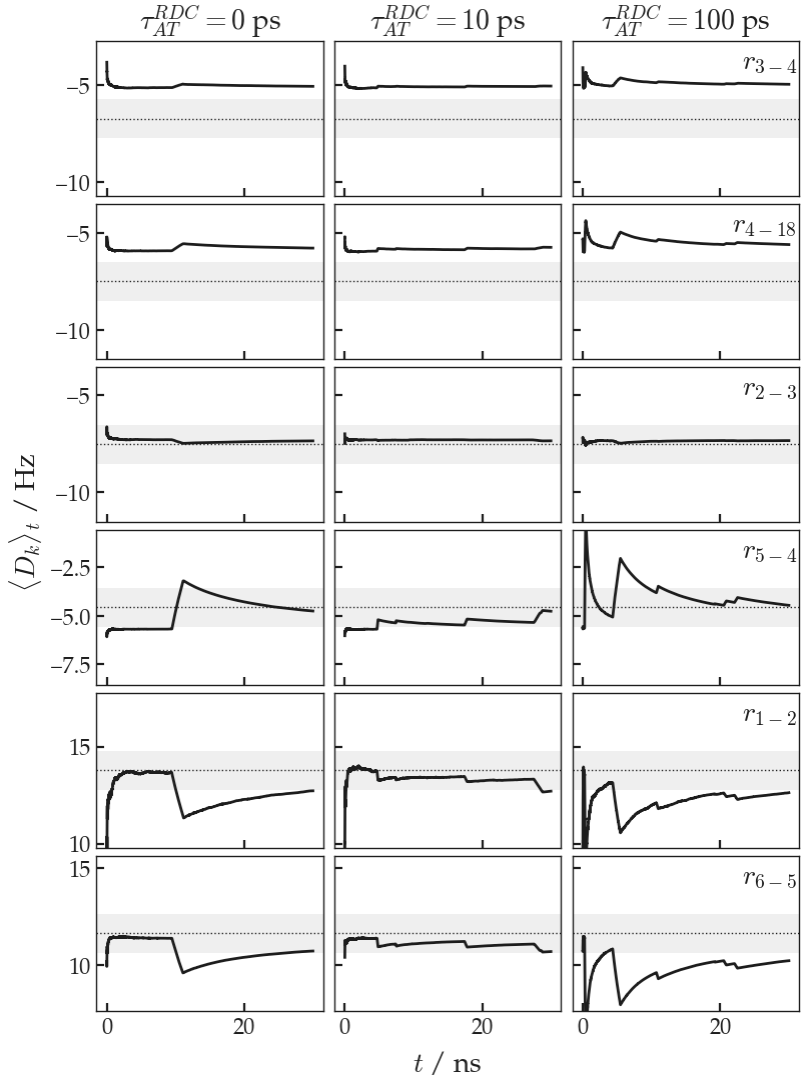


Figure 3. RDC $< D_{k_1 k_2} >_t$ values (Hz) as function of time *t* obtained for cyclo-octane as calculated from 24 bond-vector RDC-restraining *AT rSD* simulations with γ^{SD} = 0.24 ps^{-1} for all 24 bond vectors $\vec{r}_{k_1 k_2}$ (k_1-k_2), see Figure 1. The *AT* RDC-restraining function parameter values are K^{RDC} = **2 kJmol^{-1}Hz^{-2}** and τ_D^{RDC} = **100 ps** (solid lines), τ_{AT}^{RDC} = 0, 10, 100 ps (columns), and ΔD^0 = 1 Hz. The $D_{k_1 k_2}^0$ target values (dotted lines) were generated in *bSD* simulations[23] with K^{bias} = 0.2 kJmol^{-1} and θ_{bias}^0 = 0°. The area $D_k^0 \pm \Delta D^0$ is shaded.

Six RDCs (rows) are shown (backbone 3-4 and 4-18; first side chain: 2-3 and 5-4; second side chain: 1-2, 6-5). In all simulations the GROMOS force field (***GR***) was used.

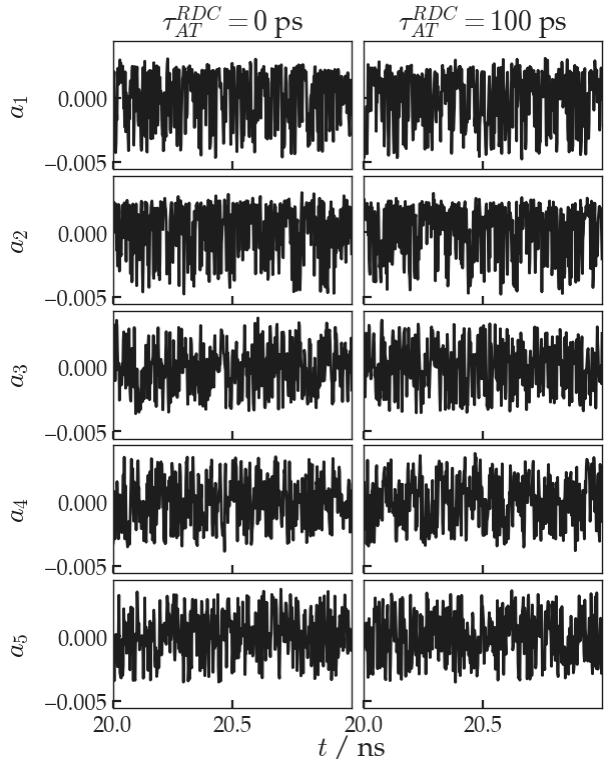


Figure 4. Values of the five quantities a_m (m = 1, 2,…, 5, rows) determining the five alignment-tensor elements as function of time t (20-21 ns) for cyclo-octane as calculated from 24 bond-vector RDC-restraining *AT rSD* simulations with γ^{SD} = 0.24 ps^{-1} for all 24 bond vectors $\vec{r}_{k_1k_2}$(k_1-k_2), see Figure 1. The *AT* RDC-restraining function parameter values are K^{RDC} = **0.01 kJmol^{-1}Hz^{-2}**, τ_D^{RDC} = **0 ps**, τ_{AT}^{RDC} = 0, 100 ps (columns), and ΔD^0 = 1 Hz. The $D^0_{k_1k_2}$ target values were generated in *bSD* simulations[23] with K^{bias} = 0.2 kJmol^{-1} and θ^0_{bias} = 0°. In all simulations the GROMOS force field (***GR***) was used.

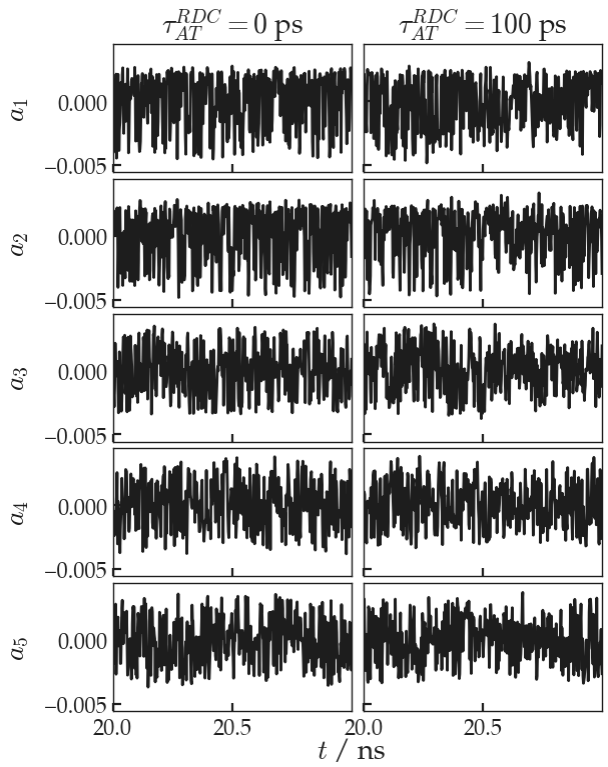


Figure 5. Values of the five quantities a_m (m = 1, 2,…, 5, rows) determining the five alignment-tensor elements as function of time t (20-21 ns) for cyclo-octane as calculated from 24 bond-vector RDC-restraining *AT rSD* simulations with γ^{SD} = 0.24 ps^{-1} for all 24 bond vectors $\vec{r}_{k_1k_2}$(k_1-k_2), see Figure 1. The *AT* RDC-restraining function parameter values are K^{RDC} = **2 kJmol^{-1}Hz^{-2}**, τ_D^{RDC} = **100 ps**, τ_{AT}^{RDC} = 0, 100 ps (columns), and ΔD^0 = 1 Hz. The $D^0_{k_1k_2}$ target values were generated in *bSD* simulations[23] with K^{bias} = 0.2 kJmol^{-1} and θ^0_{bias} = 0°. In all simulations the GROMOS force field (***GR***) was used.

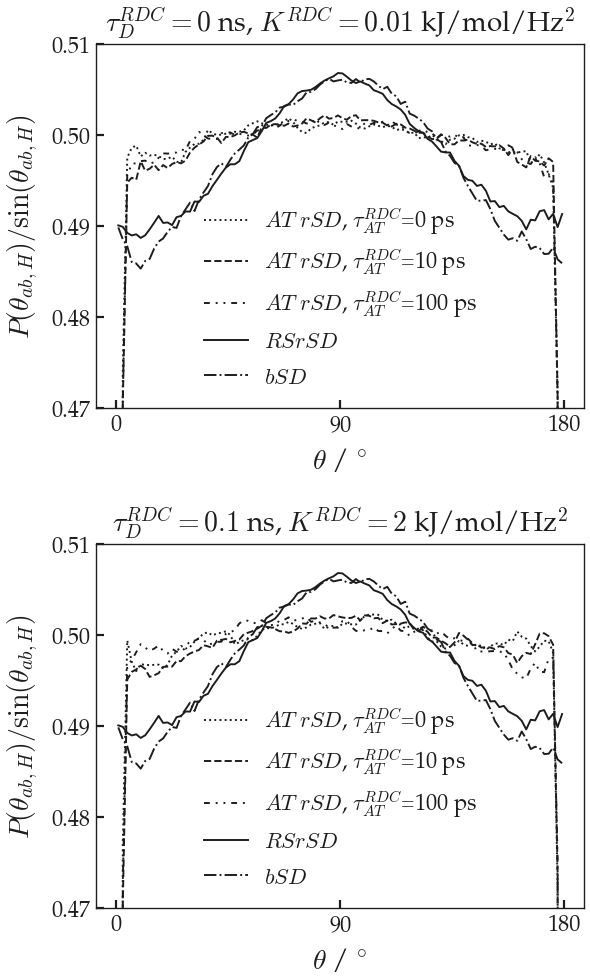


Figure 6. Angular distribution $P(\theta_{ab,H})/\sin(\theta_{ab,H})$ of the angle $\theta_{ab,H}$ between the direction of the magnetic field ($\vec{H}$) and the vector $\vec{r}_{ab}$ connecting atoms a = 11 and b = 4 (large arrow in Figure 1) obtained for cyclo-octane as calculated from a *bSD* simulation[23] (γ^{SD} = 0.24 ps^{-1}, t^{SD} = 20 μs) and from 24 bond-vector RDC-restraining *MRS*[23] (t^{SD} = 20 μs) and *AT rSD* (t^{SD} = 20 μs) simulations for all 24 bond vectors $\vec{r}_{k_1k_2}$(k_1-k_2), see Figure 1. Dot-dashed lines: orientation-biasing *bSD* simulations. Solid lines: *MRS rSD* simulations. Dotted lines: *AT rSD* simulations with τ_{AT}^{RDC} = 0 ps; dashed lines: τ_{AT}^{RDC} = 10 ps; dot-dot-dashed lines: τ_{AT}^{RDC} = 100 ps. The $D_{k_1k_2}^0$ target values were generated in *bSD* simulations with K^{bias} = 0.2

kJmol^{-1} and θ^0_{bias} = 0°. The *MRS* RDC-restraining function parameter values are K^{RDC} = 2 kJmol^{-1}Hz^{-2}, τ_θ^{RDC} = 1 ns, and ΔD^0 = 1 Hz. In the *AT rSD* simulations the restraining function parameter values are K^{RDC} = **0.01 kJmol^{-1}Hz^{-2}**, τ_D^{RDC} = **0 ps** (upper panel) or K^{RDC} = **2 kJmol^{-1}Hz^{-2}**, τ_D^{RDC} = **100 ps** (lower panel), and ΔD^0 = 1 Hz. In both *bSD* and *rSD* simulations the GROMOS force field (***GR***) was used.

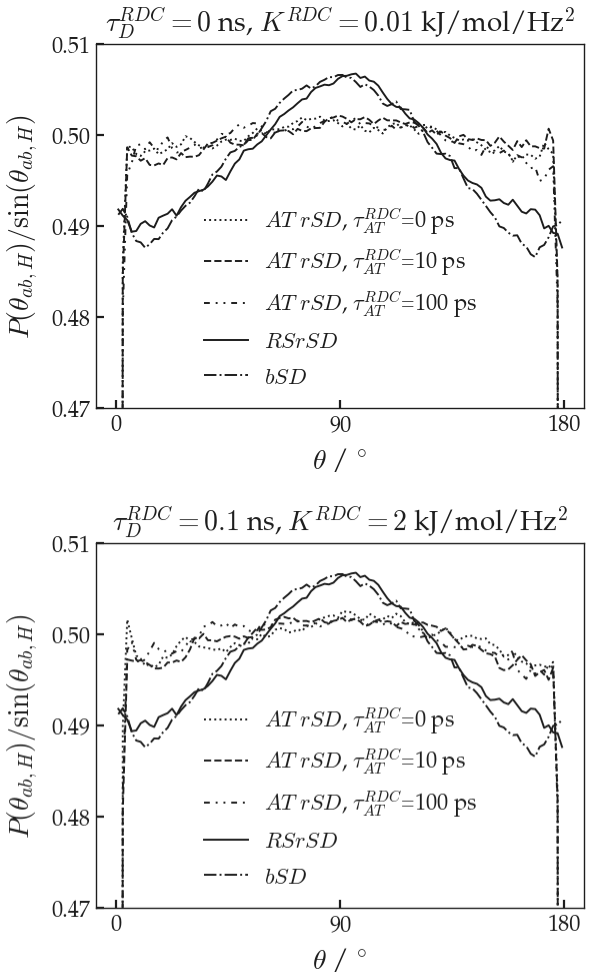


Figure 7. Angular distribution $P(\theta_{ab,H})/\sin(\theta_{ab,H})$ of the angle $\theta_{ab,H}$ between the direction of the magnetic field ($\vec{H}$) and the vector $\vec{r}_{ab}$ connecting atoms a = 11 and b = 4 (large arrow in Figure 1) obtained for cyclo-octane as calculated from a *bSD* simulation[23] (γ^{SD} = 0.24

ps^{-1}, t^{SD} = 20 μs) and from 24 bond-vector RDC-restraining *MRS*[23] (t^{SD} = 20 μs) and *AT rSD* (t^{SD} = 20 μs) simulations for all 24 bond vectors $\vec{r}_{k_1k_2}$(k_1-k_2), see Figure 1. Dot-dashed lines: orientation-biasing *bSD* simulations. Solid lines: *MRS rSD* simulations. Dotted lines: *AT rSD* simulations with τ_{AT}^{RDC} = 0 ps; dashed lines: τ_{AT}^{RDC} = 10 ps; dot-dot-dashed lines: τ_{AT}^{RDC} = 100 ps. The $D_{k_1k_2}^0$ target values were generated in *bSD* simulations with K^{bias} = 0.2 kJmol^{-1} and θ_{bias}^0 = 0°. The *MRS* RDC-restraining function parameter values are K^{RDC} = 2 kJmol^{-1}Hz^{-2}, τ_θ^{RDC} = 1 ns, and ΔD^0 = 1 Hz. In the *AT rSD* simulations the restraining function parameter values are K^{RDC} = **0.01 kJmol^{-1}Hz^{-2}**, τ_D^{RDC} = **0 ps** (upper panel) or K^{RDC} = **2 kJmol^{-1}Hz^{-2}**, τ_D^{RDC} = **100 ps** (lower panel), and ΔD^0 = 1 Hz. In both *bSD* and *rSD* simulations the GROMOS force field without torsional-angle terms (***GRnt***) was used.

For Table of Contents Only

